Published in final edited form as:
Mol Pharm. 2013 March 4; 10(3): 831–847. doi:10.1021/mp3005885.

Multifunctional gold nanoparticles for diagnosis and therapy of disease

Aneta J. Mieszawska[1], **Willem J. M. Mulder**[1,2], **Zahi A. Fayad**[1], and **David P. Cormode**[3]
David P. Cormode: david.cormode@uphs.upenn.edu

[1]Translational and Molecular Imaging Institute and Imaging Science Laboratories, Mount Sinai School of Medicine, One Gustave L. Levy Place, New York, New York 10029, USA [2]Department of Experimental Vascular Medicine, Academic Medical Center, Amsterdam, The Netherlands [3]Radiology Department, University of Pennsylvania, 3400 Spruce Street, 1 Silverstein, Philadelphia, PA 19104, USA, tel: 215-746-1382, fax: 215-662-7868

Abstract

Gold nanoparticles (AuNPs) have a number of physical properties that make them appealing for medical applications. For example, the attenuation of X-rays by gold nanoparticles has led to their use in computed tomography imaging and as adjuvants for radiotherapy. AuNPs have numerous other applications in imaging, therapy and diagnostic systems. The advanced state of synthetic chemistry of gold nanoparticles offers precise control over physicochemical and optical properties. Furthermore gold cores are inert and are considered to be biocompatible and non-toxic. The surface of gold nanoparticles can easily be modified for a specific application and ligands for targeting, drugs or biocompatible coatings can be introduced. AuNPs can be incorporated into larger structures such as polymeric nanoparticles or liposomes that deliver large payloads for enhanced diagnostic applications, efficiently encapsulate drugs for concurrent therapy or add additional imaging labels. This array of features has led to the afore-mentioned applications in biomedical fields, but more recently in approaches where multifunctional gold nanoparticles are used for multiple methods, such as concurrent diagnosis and therapy, so called theranostics. The following review covers basic principles and recent findings in gold nanoparticle applications for imaging, therapy and diagnostics, with a focus on reports of multifunctional AuNPs.

Keywords

nanoparticles; multimodality; imaging; gold; theranostics; diagnostics

INTRODUCTION

Nanoscale structures can exhibit widely different properties to bulk materials or small molecules, which renders them applicable in the fields of medical imaging and therapy.[1–4] For example, the absorbance and fluorescence of gold nanoparticles (AuNPs) is much greater compared with bulk gold, and can be tuned from the visible to the near infrared (NIR) region by changing nanostructure size and morphology.[5–7] Tissue absorbs light weakly in the NIR window, making this window ideal for optically based applications. These appealing properties have resulted in an outburst of efforts to explore synthetic routes to produce gold nanostructures of different shapes, examples of which are shown in Figure 1A. Another highly useful feature is the electromagnetic field enhancement by sharp and

Correspondence to: David P. Cormode, david.cormode@uphs.upenn.edu.

spiky edges of the nanostructures, such as stars or nanorods, which can be used in surface enhanced Raman spectroscopy imaging.[8–11] The optical scattering of AuNPs can be harnessed to detect them with a variety of microscopy methods.[12] AuNPs absorb X-rays strongly and can thus be used as contrast agents for X-ray based imaging techniques and as adjuvants for radiotherapy.[13, 14] Moreover, AuNPs can transform absorbed light into heat, resulting in localized temperature rises,[6, 15–17] which can be used to provide contrast for photoacoustic imaging[18–20] or for photothermal therapy.[17, 21–34]

Further therapeutic applications are as drug or gene delivery vehicles and, in the case of AuNPs formed from Au-198, as radiotherapeutics.[35–47] Due to these properties, AuNPs are now widely explored for their potential as diagnostic or therapeutic agents in a variety of medical fields. Furthermore, the successes of these agents has led to FDA-approvals for AuNP-based in vitro diagnostic systems and clinical trials of AuNPs as cancer and cardiovascular treatments.[48–53]

Nanoparticle multifunctionality is accomplished by combining different properties for imaging, targeting, or therapeutic delivery into one single platform. Such multifunctional platforms can serve as imaging reporters that provide complementary information or as theranostic agents, i.e. probes with concurrent imaging and therapeutic features. In the case of AuNPs, multifunctional approaches can simultaneously exploit multiple properties of the gold core, such as contrast for computed tomography (CT) imaging and the photothermal effect for therapy.[54] Alternatively, one of the effects could come from another substance incorporated into the same platform as gold cores. An example, is the use of AuNPs to deliver drugs and optical imaging of the gold cores to track delivery.[55] In this review we will briefly discuss AuNP synthesis, before surveying their abovementioned imaging, therapeutic and in vitro diagnostic applications. We will emphasize examples where multifunctional AuNPs have been used and highlight FDA-approved applications and clinical trials of AuNPs.

AUNP SYNTHESIS AND STRUCTURE

The most widely applied and simplest methods to produce AuNPs use chemical reduction of gold salt to metallic gold in the presence of a capping ligand, with the Turkevich and Brust-Schiffrin methods being the standards for aqueous and organic-based synthesis, respectively.[56, 57] In the Turkevich method, gold chloride is dissolved in water, heated to boiling point and sodium citrate is added, causing the gold salt to be reduced and gold cores to be formed.[57] The reaction results in water-soluble, citrate capped AuNPs whose size can be tuned from 15–150 nm.[58] They are not stable in saline solutions, and require coating substitution for biological applications (*vide infra*).[50] In the Brust-Schiffrin method, gold chloride is transferred from water to toluene via use of a phase transfer chemical.[56] A thiol such as dodecanethiol is added to act as a capping ligand. Sodium borohydride in water is added to reduce the gold. The AuNPs produced are highly stable, range in size from 1–5 nm and are soluble in non-polar solvents.[59] Use in biological media requires, therefore, ligand exchange[46] or additional coating with amphiphilic polymers or lipids.[60]

Other synthetic approaches include physical approaches such as microwaves and UV irradiation to nucleate the AuNPs or biological routes, so called green syntheses, with plant extracts or microorganism assisted formation of the nanostructures.[61, 62] Variations of these methods include seeded growth, where previously synthesized AuNPs are used as seeds to nucleate further growth of gold into other shapes. This is usually accomplished in the presence of surfactants and mild reducing agents or with templates.[63] Seeded growth is readily used to produce multi-shaped gold nanostructures such as rods, triangles,[64] cubes,[65] platelets or stars.[66]

Gold nanostructures are synthesized with different capping ligands that provide their solubility in aqueous or organic solvents, grant stability, and prevent aggregation. Although gold nanostructures have a rather inert and unreactive noble metal core, their biological applications often require further surface functionalization to assure high biocompatibility and low cytotoxicity.[67] Gold surfaces react easily with thiol (SH) groups forming stable Au:S bonds.[68] Therefore, thiolated ligands can be used to introduce targeting moieties, different functional groups for further reactions, or drug molecules, among other options.[69] One of the most important requirements for biological applications is a modification of the nanostructure surface with a biocompatible coating to reduce uptake by the reticuloendothelial system and prevent nonspecific binding to biological substances.[70]

A variety of coating methods have been proposed to increase the biocompatibility of AuNPs, such as ligand substitution, amphiphile coating or embedding in a carrier matrix.[67] The most widely applied coating polymer is polyethylene glycol (PEG), which is neutral in charge and highly hydrophilic, thereby preventing nonspecific protein adsorption on the nanoparticle surface, uptake by the reticuloendothelial system and providing lengthened blood circulation times.[71–73] Other examples include polyelectrolyte layer-by-layer wrapping, coating with proteins such as bovine serum albumin[74] or silica[75] coatings. AuNPs can also be incorporated into larger particles made of polymers or lipids, such as liposomes,[76] micelles[77], PLGA nanoparticles[78] or dendrimers Figure 1B.[79, 80] This approach facilitates the integration of multiple components, such as additional diagnostic or therapeutic materials, giving a route to engineer complex multifunctional nanoparticle platforms and broadening the applications of AuNPs. A generalized schematic of a AuNP for in vivo use is schematically depicted in Figure 1C.

AuNP targeting can be achieved in a passive fashion, where long circulating AuNPs can accumulate in cancers by penetrating the leaky tumor vasculature. This is known as the enhanced permeability and retention (EPR) effect.[81] Alternatively, AuNPs can be targeted to specific cell types, receptors or proteins via attachment of targeting ligands such as antibodies, proteins, peptides, aptamers and small molecules.[12, 55, 82, 83]

IMAGING

X-ray based imaging

The high atomic number and electron density of Au leads to efficient absorption of X-ray irradiation, superior to conventional iodine-based contrast agents currently used in the clinic,[13] especially at higher X-ray tube voltages, such as 120 and 140 kV. Additionally, AuNPs can offer longer circulation times than conventional agents, enabling prolonged imaging, targeting to specific cell types or other ligands and cell tracking.[82, 84, 85] Also, the payloads of AuNPs in biocompatible carriers can be precisely controlled.[78] These properties, along with the biocompatibility of gold compared with other elements that also strongly attenuate X-rays, has resulted in the exploration of AuNPs as contrast agents for X-ray based imaging techniques such as computed tomography (CT).[79, 80, 86–99]

For example, Cai et al studied the in vivo CT contrast performance of 38 nm PEG-coated AuNP as a blood-pool contrast agent for X-ray computed tomography in mice.[85] AuNPs were injected at a 493 mg Au/kg dose into mice, which were then scanned with a microCT. Long-lasting enhancements in contrast were observed in the blood vessels of the mice, with a 100 HU increase in attenuation still apparent at 24 hours post-injection. In comparison, the contrast arising from similar doses of conventional X-ray contrast agents abates within a couple of minutes. Kim et al. investigated AuNPs conjugated to a prostate-specific membrane antigen (PSMA) aptamer for specific targeting of PSMA on prostate cancer cells.[98] They used a clinical CT scanner to detect specific accumulation of the AuNPs in

these cells and when doxorubicin was additionally incorporated to the AuNP formulation they observed cancer cell death.

The addition of other contrast generating substances to Au nanostructures can generate multimodality probes that provide contrast for CT as well as other imaging techniques such as magnetic resonance imaging (MRI) or fluorescence.[100] For instance, Alric et al. developed Au nanoparticles coated with a Gd chelate for both CT and MRI (Figure 2A).[101] Examples of the contrast produced by Au-Gd nanoparticles in synchrotron radiation CT (SRCT) and MRI are shown in Figure 2A. Comparison of both SRCT and MR images of a rat taken before and after injection of the Au-Gd nanoparticles showed contrast in the kidneys, bladder and urine (Figure 2B). Analysis of the SRCT images and ex vivo ICP-MS analyses revealed urinary excretion and low accumulation in the spleen, heart, brain, liver and lungs confirming the platform's applicability as a blood pool contrast agent.

Advancements in detector technology have allowed the development of spectral CT, a technique that is currently in experimental testing.[102] Spectral CT allows multicolor imaging through splitting of the X-ray beam into six components based on the energy, enabling discrimination of different materials, which is dependent on the characteristic, energy-dependent X-ray attenuation profile of the material. The technique was applied by Cormode et al. to image and distinguish Au nanoparticles accumulated in macrophages in atherosclerotic plaques, iodine in vasculature, as well as calcified material, simultaneously.[103] As these nanoparticles have the fluorophore Rhodamine incorporated, in addition to electron microscopy, their localization in macrophages was detected by immunofluorescence as well.

Spectral CT imaging has also been done with gold nanoclusters targeted with antibodies via an avidin-biotin linkage to fibrin.[104] This was used for specific detection of clots created in vitro. Furthermore, sentinel lymph nodes could be identified following injection of gold nanoclusters into the foot of the mouse. Bismuth and ytterbium based nanoparticles, can also be specifically detected with spectral CT and have been targeted to fibrin, for thrombus detection.[105, 106]

Fluorescence imaging

The fluorescence of bulk gold, first observed by Mooradian in 1969[107], is very weak with a quantum yield in the order of 10^{-10}. Strikingly, strong fluorescence with a quantum yield of up to 10^{-3} is observed in AuNPs such as rods or shells.[108–116] Such fluorescence can be readily applied in the biomedical field, especially as it can be tuned to the NIR window (650–900 nm), a region of the electromagnetic spectrum where light penetrates tissues relatively well.[117–119] Au nanorods (AuNRs) exhibit transverse and longitudinal plasmon resonance bands that originate from the oscillation of the surface electrons along the x- and y-axis, respectively. For a given diameter, when the aspect ratio of the rod increases, the transverse band remains unchanged while the longitudinal band shifts to the red. For example, Mohamed et al. found that AuNRs with an aspect ratio of 2 had an emission maximum of 540 nm, while increasing the aspect ratio to 5.4 led to an emission maximum of 740 nm.[120] These fluorescence properties have found use in DNA biosensing.[121] To that end, Li et al. have functionalized AuNRs with DNA sequences.[121] When complementary sequences were added, the AuNRs aggregate and the fluorescence signal decreased. This process was reversed upon heating the AuNRs and disaggregation. Tang et al. used AuNR for labeling of mouse intestinal blood vessels to study the morphology of the vasculature using NIR confocal microscopy.[122]

Park et al. were able to image the 3D distribution of luminescent gold nanoshells (AuNS) in murine tumors using two-photon induced photoluminescence.[123] The AuNS were coated

with polyethylene glycol and accumulated in the tumor via the EPR effect. In addition to intrinsic fluorescence, AuNPs can be made fluorescent by the addition of organic dyes. For example, Cormode et al. used this strategy to create a AuNP based probe that provides contrast for three imaging modalities, as depicted in Figure 3A. The Au nanocrystal core (CT label) was coated with a phospholipid mixture that included Rhodamine for fluorescence as well as Gd for MRI contrast.[82] The contrast produced by this nanoparticle for the three modalities is shown in Figure 3B–C. The protein component of high-density lipoprotein was incorporated into the phospholipid coating, which provided structural integrity as well specificity for macrophages in atherosclerotic plaques, as indicated in Figure 3D–E.

Surface enhanced Raman spectroscopy imaging

Raman spectroscopy is a technique used to study molecular vibrations, rotations and other processes. Raman spectra are highly complex, and can be used as “fingerprints” of molecules, thus giving the chemical composition of a sample. Although highly specific, Raman spectroscopy is limited by its low sensitivity, since only one photon in 10^8 is Raman scattered. Absorption upon AuNP or other metal surfaces enhances the intensity of the vibrational spectra of Raman active molecules by several orders of magnitude.[124] This discovery has led to emergence of a new technique called surface enhanced Raman spectroscopy (SERS). This phenomenon, which is widely observed and studied using AuNPs, is thought to be due to an electromagnetic field close to the particle surface produced by the presence of a localized surface plasmon resonance (the collective oscillation of surface electrons).[125–128] The strongest electromagnetic field enhancement occurs at sharp nanostructure edges like AuNR tips and between aggregated colloids. Also, the surface plasmon absorption of Au nanostructures can be tuned into the NIR, thus avoiding absorption of excitation light by biological samples and limiting the interference for the SERS signal.[129] Therefore Au nanostructures are attractive as labels for flow cytometry[130] and as contrast agents for biological SERS imaging.[131–134,135–137,138]

Fujita’s group investigated the entry of AuNPs into living cells with SERS imaging. Macrophage cells were incubated with 50 nm Au nanoparticles and imaged using a Raman microscope. SERS signals were observed from biomolecules near the nanoparticle surfaces. Nanoparticle movement inside the cell could be followed with high spatial resolution. Fluctuations in the Raman signal over time were attributed to the adsorption/desorption of biomolecules to the nanoparticle surface.[139] Similarly, Eliasson et al. demonstrated the SERS discrimination between several intracellular components in living cells using SERS.[140] Single human lymphocytes were incubated with AuNPs and Rhodamine 6G as a model analyte. SERS imaging allowed for the identification of Rhodamine 6G probe within the cell as well as spectra corresponding to DNA and nucleotides.

Qian et al. reported a SERS contrast agent where a reporter molecule (malachite green) was adsorbed onto the surface of 60 nm AuNPs.[141] An additional coating of PEG was applied. The contrast arising from these nanoparticles was found to be 200 times that of quantum dots, another type of nanoparticle proposed for optical contrast. The authors demonstrated that subcutaneous injections of the AuNPs into the flank of a mouse could be detected using a SERS microscope. Furthermore, targeting the Au-NPs with an antibody against anti-epidermal growth factor receptor (EGFR) resulted in enhanced binding to tumor cells that overexpressed this receptor. Targeted and non-targeted AuNPs were injected into tumor bearing mice and both SERS spectra and ICP-MS confirmed a greater accumulation at 5 hours post-injection.

Kircher et al. employed a multifunctional approach combining SERS, MRI and photoacoustics, where a AuNP-based platform was used to image brain tumors and

accurately guide surgery, offering improved identification of the tumor margins.[142] The nanoparticle consisted of a 60 nm gold core coated with a highly Raman active molecule *trans*-1,2-bis(4-pyridyl)-ethylene and a 30 nm thick silica shell. The silica surface was further modified with Gd^{3+} chelates. In this design the AuNPs served as a contrast agent for photoacoustic imaging and the amplifier for the SERS Raman tag, while Gd^{3+} provides contrast for MRI. The photoacoustic imaging gives high spatial resolution combined with highly sensitive SERS imaging led to detailed identification of the tumor outline. The in vivo detection threshold for the nanoparticles was found to be very low, in the 50 pM range. After tail-vein injection of the agent in a tumor mouse model, the MRI contrast-to-noise ratio of the tumor increased from 2.2 ± 0.3 to 14.0 ± 1.9, the photoacoustic signal increased by 75 % and the SERS signal of the agent was detected with an SNR of 11.1. Use of this agent improved the success of resections in removing all tumor tissue.

Photoacoustic imaging

In photoacoustic imaging, the subject is irradiated with light, which results in localized heating, and a small expansion of tissue, causing a sound wave. Use of short laser pulses generates sound waves in the ultrasonic frequency range.[143, 144] Photoacoustic imaging is advantageous compared to some other imaging techniques, as the radiation used is non-ionizing and the use of ultrasound as the output results in higher spatial resolution compared to optical methods due to the lower scattering of ultrasound in tissue. Since different types of biological tissues have different light absorption coefficients, this imaging modality can discriminate between tissues and has a penetration depth in the centimeter range with sub-millimeter spatial resolution.[19, 145, 146] Due to their aforementioned strong absorption of light, AuNP have been explored as contrast agents for photoacoustic imaging.[20] In this case also, using light in the NIR window is advantageous.[147–151] The range of gold nanostructures whose absorbance is adjustable to the NIR region by size or morphology (e.g. cages,[152–154] nanospheres,[155] and nanorods[155]), have been applied for this imaging technique.[18, 143, 156–158]

Agarwal et al. published one of the earliest examples of gold nanoparticles used as contrast agents for photoacoustic imaging.[159] In this study gels containing AuNR were implanted in the hind limb of a mouse and imaged with a photoacoustic system. Lu et al. tested PEG-coated AuNSs for photoacoustic tomography of the vasculature in mice.[160] The AuNSs were ~ 50 nm in diameter with an absorption peak precisely tuned to 800 nm. Photoacoustic imaging using these nanoparticles resulted in very high spatial resolution images of the brain vasculature, with capillaries detected of diameter as little as 100 μm. In another example Wang et al. employed PEGylated AuNPs as a contrast agent to detect macrophages in atherosclerotic plaques ex vivo. Endocytosis of AuNPs by macrophages caused AuNP aggregation inside the cells and a resultant red-shift in absorption due to plasmon resonance coupling. This allowed discrimination of the AuNPs inside macrophages from free AuNPs via the use of irradiation of different wavelengths.[161] Pan et al. have developed a photoacoustic contrast agent for intravascular imaging based on an almond oil emulsion encapsulated in phospholipids carrying multiple 2–4 nm AuNPs [162, 163] The surface of the nanoparticle was decorated with the biotin ligand, which allowed targeting of fibrin via the use of an avidin labeled antibody. In vitro experiments revealed marked targeting to fibrin-rich clots, as compared to non-targeted nanoparticles.[162] Non-targeted nanoparticles were used as a vascular phase agent and were found to increase the photoacoustic signal amplitude of the blood vessels of rats by 60%, when injected at a 3 Au mg/kg dose.[164] In a further experiment, these AuNPs, when targeted to the $\alpha_v\beta_3$-integrin, were shown to specifically accumulate in a mouse matrigel model of angiogenesis (a process where the $\alpha_v\beta_3$-integrin is overexpressed).[163]

The Emelianov group used combined photoacoustic and ultrasound imaging to perform in vivo tracking of mesenchymal stem cells labeled with 20 nm AuNPs.[165] Noninvasive detection of stem cells in vivo is very attractive for the optimization and monitoring of stem cell-based therapies. The labeled stem cells were embedded in a PEGylated fibrin gel, which was subsequently implanted into rats. Ultrasound provided anatomical information, while multiwavelength photoacoustic imaging was used to localize AuNP labeled cells and identify other biological components. As is shown in Figure 4, photoacoustic imaging could detect labeled cells injected in the hind limb. Furthermore, the cells could be spectrally distinguished from oxygenated hemoglobin, deoxygenated hemoglobin, and skin, as depicted in Figure 4D and H. In a multimodality approach, Qu et al. combined ultrasound, photoacoustic imaging and a technique known as magneto-motive ultrasound (MMUS) into hybrid magneto-photoacoustic (MPA) imaging.[166] MMUS employs a pulsed magnetic field to make magnetically labeled tissue rapidly vibrate, producing ultrasound waves. For this combined approach, a liposomal formulation of AuNRs and iron oxide nanoparticles was developed as contrast agents for both photoacoustics and MMUS. In vitro imaging confirmed that only liposomes loaded with AuNR and iron oxide gave contrast in both techniques. Furthermore, merging the data from both techniques gave improved contrast resolution. Kim et al. reported an unusual platform composed of carbon nanotubes upon which was grown a gold shell.[167] These structures were also found to be effective photoacoustic contrast agents and to produce heat upon irradiation, thus have potential as therapeutics via photothermal heating.

Optical imaging

AuNPs have extraordinary light scattering properties, which are not observed in non-plasmonic nanoparticles. Changes in size and shape of AuNPs also influence scattering, providing an opportunity to tune the agent to possess optimal light scattering performance. For example, the reflection coefficient and the optical cross section both increase with size, leading to more efficient light scattering by larger rather than smaller nanoparticles.[168] Additionally, compared with fluorescent probes used in optical imaging, AuNPs do not suffer from photobleaching.[169] These properties have encouraged investigations of AuNPs as contrast agents for light scattering imaging.[168, 170, 171,172]

For example, Qian et al. used dark field microscopy to image cancer cells for two cell cycles, monitoring resonant light scattering from AuNPs.[173] The strong scattering signals enabled visualization of AuNP entry to the cell nucleus (when functionalized with RGD peptides and a nuclear location sequences) or the cytoplasm (when coupled to RGD only), and their localization was traceable after cell division. The light scattering of AuNPs was used by El-Sayed et al. to discriminate cancerous cells from healthy cells.[12] 35 nm AuNPs were modified with an anti-EGFR antibody and incubated with a nonmalignant epithelial cell line and two malignant oral epithelial cell lines. The malignant cell lines over-express EGFR, in comparison with the non-malignant cells. Light scattering signals from AuNPs could easily be detected and 600 % higher signal was found in malignant compared with non-malignant cells when incubated with antibody modified AuNPs. Non-targeted AuNPs did not show a significant difference in uptake between the cell lines. Furthermore, non-targeted AuNPs seemed to aggregate within the cells, as indicated by a red-shift of their absorption maximum from 545 to 552 nm, allowing secondary spectroscopic evaluation of imaging results.

THERAPY

Drug delivery

AuNPs have a range of properties that make them suitable for drug delivery. The noble metal core is inert, contributing to low toxicity and good biocompatibility, which are requirements for biological applications.[174] The flexibility in AuNP size and shape facilitates selection of dimensions optimal for loading therapeutics such as proteins, peptides, oligonucleotides, or small drug molecules.[69, 175, 176] Additionally, high surface area and a choice of surface chemistries facilitate the loading of not only a large therapeutic cargo but also other entities such as targeting molecules, linkers, additional contrast media and so on.[177–180] AuNPs have been widely studied for application in anticancer therapy, due to the great need for new treatments in this area.[181–186] Furthermore, AuNPs can preferentially accumulate in tumors through the EPR effect.

In a simple example, Tomuleasa et al. tested three different AuNPs formulations containing either doxorubicin, cisplatin, and capecitabine, for treatment of liver cancer.[187] The drug molecules were non-covalently complexed to AuNPs coated with aspartic acid. The cell lines used were hepatocellular carcinoma cells, chemotherapy resistant hepatocellular carcinoma cells and non-cancerous liver cells. Enhanced therapeutic outcomes were observed for the cancer cells treated with AuNP-drug conjugates when compared to free drugs. Additionally, the AuNP-drug complexes were effective against the chemotherapy resistant cells.

In another study, Kumar et al. combined therapy with active targeting by functionalizing AuNPs with both therapeutic and targeting peptides.[83] The PMI peptide interferes with the p53 pathway and can thus induce cancer cell apoptosis. The CRGDK peptide binds to the neuropilin-1 receptor, which is overexpressed on cancer cells. Both peptides were covalently linked to 2 nm AuNPs. The internalizing and therapeutic effects were compared using two breast cancer cell lines: MDA-MB-321, which expresses the neuropilin-1 receptor and MCF-7S, which has low neuropilin-1 expression. Incubation with these AuNPs led to stronger in vitro toxicity for MDA-MB-321 cells than MCF-7S. These and other experiments proved neuropilin-1 mediated recognition and internalization.

Heo et al. reported a complex AuNP platform that included biotin as a targeting ligand, the anticancer drug paclitaxel, Rhodamine B to facilitate fluorescence detection and PEG for enhanced biocompatibility.[55] Cyclodextrin, a well known drug-host molecule, was attached to the AuNP surface for non-covalent paclitaxel inclusion. A schematic depiction of the AuNP platform is shown in Figure 5A. Biotin was used as a targeting ligand due to the overexpression of biotin receptors on certain cancer cells. These AuNPs were evaluated using a multimodality approach in vitro with three different cancer cell lines (HeLa, A549, MG63), while fibroblasts (NIH3T3) were used as controls. After treatment with AuNPs for 24 hours, the cancer cells had half the viability rate when compared to the control cells (Figure 5B). The multiplexed AuNPs showed higher internalization, visualized by dark field microscopy and confirmed by Rhodamine B fluorescence, in all three cancer cell lines than in the control cells (Figure 5C). This is a multifunctional AuNP platform that allows concurrent therapy and diagnosis, i.e. theranostics.

Paciotti et al. developed a formulation of AuNPs, which are coated with a mixture of tumor necrosis factor (TNF) and PEG.[188] TNF has potent anti-tumor effects, but its use as a therapeutic is limited by its systemic toxicity. The authors hypothesized that use of a nanoparticle delivery system could reduce the systemic toxicity of TNF and increase its tumor accumulation. Investigations of the AuNP-TNF formulation in tumor bearing mice, found a ninefold increase in TNF accumulation in the tumor. Furthermore, reductions in

tumor growth and improvements in survivability were observed. These positive results encouraged the implementation of a phase I clinical trial using AuNP-TNF in patients with advanced solid organ tumors.[50] Doses up to 600 ug/m^2 were tested and found to be tolerable. AuNPs were detected in biopsies taken from the tumors of the patients, but not in healthy tissue. Future clinical trials are needed to evaluate the efficacy of this therapy in patients.

Nucleic acid delivery

Gene delivery is another field where AuNPs are being explored for their therapeutic potential.[189–191] The versatility and multifunctionality of AuNPs has facilitated several different approaches for encapsulation and release of nucleic acids. In a relatively straightforward approach, Lee et al. used AuNRs coated with cationic phospholipids as delivery vehicles for nucleic acid cargoes. The positively charged phospholipid surface was used to attach negatively charged DNA, RNA or siRNA oligonucleotides.[192] Internalization of AuNRs complexed with nucleic acids was observed with darkfield scattering microscopy.

Conde et al. have developed a complex AuNP platform for efficient RNAi delivery to silence the c-myc protooncogene.[193] They used a hierarchical approach, starting with cultured human cells, through invertebrates, and vertebrate (mouse) models, to select AuNP compositions that produce the most efficient therapy. The optimal formulations contained PEG chains for increased stability, RGD targeting peptides, cell penetrating TAT peptides, and siRNA either covalently or ionically attached to the nanoparticles. An elegant example of gene silencing using AuNPs as delivery agents was presented by Shim et al., shown in Figure 6.[194] The siRNA was linked with multiple AuNPs through an acid-sensitive ketal linker group, forming an aggregate (Figure 6A). The ketal linker is cleaved at low pH, releasing both the oligonucleotides and the AuNPs. Changing from an aggregate to individual particles results in a radical change in the optical properties of the AuNPs. Optical coherence tomography was used to detect this change and confirm the aggregate's disintegration at tumor relevant pH (Figure 6B). In vitro microscopy experiments on GFP expressing cells confirmed specific gene silencing under low pH conditions (Figure 6C).[194]

The optical properties of AuNPs may also be used to trigger release of nucleic acids due to strong absorption of light and resultant heating of the nanoparticle, causing the nucleic acid-nanoparticle bonds to break. Cui et al. investigated dendrimer coated AuNRs as a delivery vehicle for brcaa1-shRNA delivery into MCF7 cancer cells. Dendrimers are often used in delivery systems to increase the biocompatibility and cellular uptake. Near infrared laser irradiation triggered RNA release from AuNRs encapsulated in dendrimers that led to successful silencing of brcaa1 gene in MCF7 cells.[195] Furthermore, Wijaya et al. demonstrated the conjugation of two different DNA oligonucleotides onto the surface of AuNRs with different aspect ratios. Selective release of the DNA absorbed onto the AuNRs was accomplished with irradiation at wavelengths corresponding to the characteristic absorption band of the different AuNRs.[196]

Photothermal therapy

The property of photon absorption and conversion into thermal energy by AuNPs quickly found use in photothermal therapies, especially for cancer applications. The irradiation of AuNPs with light of the correct wavelength induces localized temperature increases, which leads to photothermal ablation of cells in the vicinity, as such temperature increases cause biomolecule denaturation and cell damage.[30, 197–202] This therapeutic approach can be highly targeted to cancer due to greater nanoparticle accumulation in tumors compared with normal tissue and selective irradiation of only the tumors. For example Chen et al. synthesized Au nanocages with tunable NIR absorption between 600–1200 nm.[203] In a

proof of principle experiment, they showed that laser irradiation of a 1ppm solution of nanocages raised water temperature by 5–10 °C, which could lead to an increase in tissue temperature from 37 to 42 °C or greater. In vivo thermography imaging of mice bearing tumors and injected with Au nanocages indicated tumor heating post laser irradiation. Nuclear imaging indicated a therapeutic effect in terms of a decrease in the metabolism in the tumors of the injected animals. Furthermore, histology revealed cell damage in the form of coagulative necrosis after laser irradiation treatment. In another approach, Wang et al. developed supramolecular assemblies of Au-NPs (Au-SA-NPs) to collectively enhance the photothermal power in the tumor cell vicinity.[204] The nanoparticles were formed from three building blocks: adamantine-grafted 2 nm Au colloids, β-cyclodextrin-grafted branched polyethylenimine, and Ad-grafted PEG. As β-cyclodextrin binds adamantine strongly, combining these building blocks led to the formation of stable Au-SA-NPs and further functionalization with the RGD peptide enabled targeting of the $\alpha_v\beta_3$ integrin receptors overexpressed on cancer cells. When applied in vitro, RGD-targeted Au-SA-NPs effectively homed to $\alpha_v\beta_3$ positive U87 glioblastoma cells, as confirmed by TEM imaging, and when the cells were irradiated with a pulsed laser the resultant was cell damage confined to the irradiation area.

Von Maltzahn et al used a theranostic approach to photothermal therapy using AuNRs to treat cancer in vivo (Figure 7A).[54] The AuNRs were coated with PEG, had long circulation times of ~ 17 hours and were found to have high light absorption, about 6 times higher than Au nanoshells. CT imaging was used to generate maps of AuNR tumor accumulation post-injection into tumor bearing mice, as shown in Figure 7B. This information enabled computational modeling of the laser irradiation needed to ablate the tumor. Increases in tumor temperature were found post-irradiation (Figure 7C). Compared to controls, this regimen was much more potent, leading to almost complete tumor ablation in vivo (Figure 7D).[54] In another approach, Park et al. enhanced photothermal therapy by combining the anti-cancer drug doxorubicin and gold into the same platform.[205] These Au coated polymeric nanoparticles loaded with doxorubicin were used in laser irradiation experiments with HeLa cells, leading to heat-induced drug release and enhanced anticancer effects.

The success of these approaches has led to evaluation of AuNPs induced photothermal therapy in clinical trials. A gold nanoshell formulation known as Auralase is being tested in patients with head and neck tumors.[51] Furthermore, two clinical trials have been performed using AuNPs in patients with coronary artery disease.[52, 53] More clinical trials will likely be initiated in this area.

Radiotherapy

Another interesting feature of AuNPs is their radiosensitizing property. Radiotherapy is widely used in cancer therapy since radiation (X-rays, **γ**-rays and fast-moving charged particles such as ions, electrons and protons) induces DNA damage, thus killing cancer cells. Following the absorption of X-rays by the tumor, there is a release of scattered photons and electrons, causing DNA damage.[206–211] Clinically, special devices are used that irradiate the tumor from a number of angles, maximizing X-ray dose in the tumor and minimizing it in healthy tissues. Lead shielding is used to further minimize dose to healthy tissue. Gold is an excellent absorber of X-ray energy and can greatly elevate the dose of absorbed irradiation, once localized in the tumor site, thus increasing the therapeutic effects of the radiation dose.

Liu et al. tested different X-ray sources on cancer cell survival with and without the presence of PEG-coated AuNPs.[14] They found that survival of cells that were exposed to X-rays in the presence of Au NPs decreased in an X-ray dose dependent fashion. In another measure of the therapeutic effect, the surviving cells had distorted morphology and abnormal distribution of organelles. Hainfeld et al. evaluated 1.9 nm, PEGylated AuNPs for

enhancement of radiotherapy in tumor bearing mice.[212] Tumor growth in mice injected with 1.35 g Au/kg and subjected to X-ray treatment was halted, whereas tumors in mice treated with X-rays alone continued to grow, albeit slower than untreated mice. Furthermore, at one year post-treatment, 86% of mice that were injected with 2.7 g Au/kg and irradiated with X-rays were still alive, a greatly increased percentage compared with controls.

In an alternative approach, AuNPs coated in ascorbic acid and formed from Au-198 salts were originally investigated for their potential as radiotherapeutics in the 1950s and 1960s.[47, 213–215] The aim in this area is that the nanoparticles will preferentially accumulate in the tumor and emit radiation which will be absorbed by the cancer cells, killing them. With the advent of improved nanoparticle synthesis methods and coating materials, this approach has been recently revived.[215] Radioactive AuNP were synthesized with an epigallocatechin-gallate coating.[47] Epigallocatechin-gallate was used as it has been shown to target prostate cancer. Dark field microscopy and transition electron microscopy were used to confirm that the particles were taken up in prostate cancer cells. When these nanoparticles were injected into the tumors of mice, the tumor growth was arrested over the next 35 days, indicating the therapeutic effect.

DIAGNOSTICS

AuNP have interesting applications in the molecular diagnostic field.[216] The development of methods for earlier detection is important to reduce the impact of diseases and to improve survival rates. AuNPs have high surface-to-volume ratios and can be functionalized to detect specific targets, offering lower detection limits and higher selectivity than conventional strategies. They have been studied to detect analytes such as gases, ions, protein markers or DNA.[217–220]

Mirkin's group were pioneers in this field and have published widely on the use of AuNPs in molecular detection systems.[218, 221–223] In a seminal work, published in 1997, they reported an AuNP system, which is composed of two populations of AuNPs.[224] Each type of AuNP is coated with different thiol-oligonucleotides. The last 15 nucleotides are complementary to one half of a target DNA sequence. When the target DNA is introduced into the system, the two types of AuNPs both bind to the DNA and aggregate. This results in a color change from red to blue, which is a well-known behavior of AuNPs. This colorimetric, AuNP-based technology has been developed into diagnostic products that are now FDA-approved. These products are used to test for Warfarin metabolism and for F5/F2/MTHFR mutations,[48, 49] amongst other applications.

This methodology has been extended in a number of different directions, for example, via conductivity-based detection of DNA using microelectrodes and Ag deposition amplification of the signal arising from the AuNPs.[225] Gold microelectrodes with 20 μm gaps were fabricated on a Si substrate were modified with "capture" oligonucleotide strands. The sensor was then exposed to "target" oligonucleotides in solution. The capture oligonucleotides contained short DNA sequences complementary to part of the target oligonucleotides, so upon binding overhanging strands are left exposed. This design allowed binding of AuNPs capped with oligonucleotides complementary to the target's overhangs, bridging the electrode gaps and decreasing the resistance across the microelectrode. Ag reduction onto the AuNPs closed the spaces between the nanoparticles and the electrodes, leading to further sharp decreases in resistance. The proposed sensor allowed for the detection of target DNA in the 50 nM to 500 fM concentration range.

Conde et al. recently reported the first quantification of mutation expression in mRNA taken directly from cancer cells, using oligonucleotide coated AuNPs.[226] No amplification of the RNA was needed. The AuNPs were modified with DNA complementary to the *BCR-ABL*

b3a2 fusion transcript mRNA, which is responsible for chronic myeloid leukemia (CML). 13 nm AuNPs were modified with thiolated oligonucleotides and exposed to total RNA isolated from several cell lines. In the absence of the target DNA, the nanoparticles did not aggregate and remained red in color. When exposed to RNA extracted from cells expressing the mutant gene, there was a visible color change, enabling easy colorimetric detection.

In another approach, Lou et al. constructed a "chemical nose" sensor based on the poly(p-phenyleneethynylene) (PPE) polymer and AuNPs, capable of distinguishing 7 different proteins.[217] The nanosensor was composed of an array of six AuNPs with different cationic coatings, each complexed with negatively charged PPE-CO_2 polymer. The PPE polymer is highly fluorescent but the fluorescence is quenched when bound to the AuNPs. The differing capping ligands used to coat the AuNP surface, provide weaker or stronger interactions with a polymer and protein analytes. Addition of protein analytes disrupts the assembly between the AuNPs and PPE-CO2 polymer resulting in fluorescence from the polymer. The protein analytes were chosen to have different sizes and charges and thus had differential binding to the AuNPs. Therefore each protein resulted in a unique fluorescent pattern from the array, enabling their distinction in a mixture. The array was tested against 52 protein samples and correctly identified the protein with 94.2% accuracy. This approach is an excellent example of exploitation of the tunability of AuNP surface chemistry to optimize performance.

CLINICAL TRIALS AND FDA APPROVAL

From the above it is clear that there has been tremendous progress in the development of AuNP for biomedical applications. The AuNP that have been approved for clinical use are used in diagnostic applications.[48, 49] The requirements for regulatory approval of diagnostic systems are relatively low, as samples are analyzed ex vivo. We expect that more such diagnostic tests will be approved in the near future. The requirements for FDA-approval of injectable AuNP are much higher, as evidenced by the relatively small number of clinical trials involving AuNP to date.[50–53] Nanoparticles are currently treated by the FDA in the same way as any other drug or imaging agent. Despite the relatively biocompatibility of gold, long-term retention of a large quantity of the injected material would likely prevent FDA-approval due to concerns over the long-term effects. Hence studying the excretion of AuNP is a key step towards a clinical trial. In applications where large doses are needed, such as CT, where doses as high 1.35 g Au/kg have been used,[86] this is absolutely crucial. In applications where the dose of gold is much lower, such as photoacoustic imaging (as low as 22.7 μg Au/kg[227]), excretion may be less crucial, as small amounts of gold are typically present and tolerated in the body.[228] Much of the work on AuNP for biomedical applications has arisen from the laboratories of scientists originally trained as chemists and who have developed the synthesis or studied the properties of AuNP.[12, 174, 223] Translation of more AuNP to the clinic will be facilitated by closer interactions between the physical scientists who are experts on AuNP and biologists and clinicians. This will drive the design of AuNP that closely address clinical problems and the biological basis of diseases.

CONCLUSIONS

AuNPs have versatile physical properties that make them suitable for many biomedical applications. Compared with small molecules, their detectability for imaging techniques can be several orders of magnitude higher, greatly lowering detection limits. Some clinical imaging techniques including CT would benefit greatly from new nanoparticle-based contrast agents that offer longer circulation times and localized accumulation at the disease site for improved diagnoses. Also, AuNP-based platforms can be used to enhance or enable a wide variety of therapies, such as drug delivery, nucleic acid delivery, photothermal ablation and radiotherapy. The ability to tune the size, shape and consequently the physical

properties of AuNPs, along with their low cytotoxicity, high biocompatibility, and range of surface chemistries makes them promising candidates for clinical use. This is borne out by AuNP-based diagnostic products now being available and FDA-approved and a number of formulations in clinical trials as therapeutics.

Acknowledgments

This work was supported by the National Heart, Lung, and Blood Institute, National Institutes of Health, as a Program of Excellence in Nanotechnology (PEN) Award, Contract #HHSN268201000045C, as well as by R01 EB009638 (Z.A.F.), R01 CA155432 (W.J.M.M.) and R00 EB012165 (D.P.C.).

References

1. Biju V, Itoh T, Anas A, Sujith A, Ishikawa M. Semiconductor quantum dots and metal nanoparticles: syntheses, optical properties, and biological applications. Anal Bioanal Chem. 2008; 391(7):2469–95. [PubMed: 18548237]
2. Sau TK, Rogach AL. Nonspherical noble metal nanoparticles: colloid-chemical synthesis and morphology control. Adv Mater. 2010; 22(16):1781–804. [PubMed: 20512953]
3. Tokonami S, Yamamoto Y, Shiigi H, Nagaoka T. Synthesis and bioanalytical applications of specific-shaped metallic nanostructures: a review. Anal Chim Acta. 2012; 716:76–91. [PubMed: 22284881]
4. Lu Y, Chen W. Sub-nanometre sized metal clusters: from synthetic challenges to the unique property discoveries. Chem Soc Rev. 2012; 41(9):3594–623. [PubMed: 22441327]
5. Payne EK, Shuford KL, Park S, Schatz GC, Mirkin CA. Multipole plasmon resonances in gold nanorods. J Phys Chem B. 2006; 110(5):2150–4. [PubMed: 16471797]
6. Hu M, Petrova H, Chen J, McLellan JM, Siekkinen AR, Marquez M, Li X, Xia Y, Hartland GV. Ultrafast laser studies of the photothermal properties of gold nanocages. J Phys Chem B. 2006; 110(4):1520–4. [PubMed: 16471708]
7. Fleischer M, Zhang D, Braun K, Jager S, Ehlich R, Haffner M, Stanciu C, Horber JK, Meixner AJ, Kern DP. Tailoring gold nanostructures for near-field optical applications. Nanotechnology. 2010; 21(6):065301. [PubMed: 20057031]
8. Kneipp J, Kneipp H, Rice WL, Kneipp K. Optical probes for biological applications based on surface-enhanced Raman scattering from indocyanine green on gold nanoparticles. Anal Chem. 2005; 77(8):2381–5. [PubMed: 15828770]
9. Stokes RJ, Macaskill A, Lundahl PJ, Smith WE, Faulds K, Graham D. Quantitative enhanced Raman scattering of labeled DNA from gold and silver nanoparticles. Small. 2007; 3(9):1593–601. [PubMed: 17647254]
10. Kneipp J, Li X, Sherwood M, Panne U, Kneipp H, Stockman MI, Kneipp K. Gold nanolenses generated by laser ablation-efficient enhancing structure for surface enhanced Raman scattering analytics and sensing. Anal Chem. 2008; 80(11):4247–51. [PubMed: 18439029]
11. Rycenga M, Wang Z, Gordon E, Cobley CM, Schwartz AG, Lo CS, Xia Y. Probing the photothermal effect of gold-based nanocages with surface-enhanced Raman scattering (SERS). Angew Chem Int Ed Engl. 2009; 48(52):9924–7. [PubMed: 20014343]
12. El-Sayed IH, Huang X, El-Sayed MA. Surface plasmon resonance scattering and absorption of anti-EGFR antibody conjugated gold nanoparticles in cancer diagnostics: applications in oral cancer. Nano Lett. 2005; 5(5):829–34. [PubMed: 15884879]
13. Galper MW, Saung MT, Fuster V, Roessl E, Thran A, Proksa R, Fayad ZA, Cormode DP. Effect of computed tomography scanning parameters on gold nanoparticle and iodine contrast. Invest Radiol. 2012; 47(8):475–81. [PubMed: 22766909]
14. Liu CJ, Wang CH, Chen ST, Chen HH, Leng WH, Chien CC, Wang CL, Kempson IM, Hwu Y, Lai TC, Hsiao M, Yang CS, Chen YJ, Margaritondo G. Enhancement of cell radiation sensitivity by pegylated gold nanoparticles. Phys Med Biol. 2010; 55(4):931–45. [PubMed: 20090183]
15. Chen X, Chen Y, Yan M, Qiu M. Nanosecond photothermal effects in plasmonic nanostructures. ACS Nano. 2012; 6(3):2550–7. [PubMed: 22356648]

16. Chen H, Shao L, Ming T, Sun Z, Zhao C, Yang B, Wang J. Understanding the photothermal conversion efficiency of gold nanocrystals. Small. 2010; 6(20):2272–80. [PubMed: 20827680]
17. Huang X, Kang B, Qian W, Mackey MA, Chen PC, Oyelere AK, El-Sayed IH, El-Sayed MA. Comparative study of photothermolysis of cancer cells with nuclear-targeted or cytoplasm-targeted gold nanospheres: continuous wave or pulsed lasers. J Biomed Opt. 2010; 15(5):058002. [PubMed: 21054128]
18. Chen LC, Wei CW, Souris JS, Cheng SH, Chen CT, Yang CS, Li PC, Lo LW. Enhanced photoacoustic stability of gold nanorods by silica matrix confinement. J Biomed Opt. 2010; 15(1): 016010. [PubMed: 20210456]
19. Emelianov SY, Li PC, O'Donnell M. Photoacoustics for molecular imaging and therapy. Phys Today. 2009; 62(8):34–39. [PubMed: 20523758]
20. Yang X, Stein EW, Ashkenazi S, Wang LV. Nanoparticles for photoacoustic imaging. Wiley Interdiscip Rev Nanomed Nanobiotechnol. 2009; 1(4):360–8. [PubMed: 20049803]
21. Kuo WS, Chang YT, Cho KC, Chiu KC, Lien CH, Yeh CS, Chen SJ. Gold nanomaterials conjugated with indocyanine green for dual-modality photodynamic and photothermal therapy. Biomaterials. 2012; 33(11):3270–8. [PubMed: 22289264]
22. Young JK, Figueroa ER, Drezek RA. Tunable nanostructures as photothermal theranostic agents. Ann Biomed Eng. 2012; 40(2):438–59. [PubMed: 22134466]
23. Rejiya CS, Kumar J, Raji V, Vibin M, Abraham A. Laser immunotherapy with gold nanorods causes selective killing of tumour cells. Pharmacol Res. 2012; 65(2):261–9. [PubMed: 22115972]
24. Samim M, Prashant CK, Dinda AK, Maitra AN, Arora I. Synthesis and characterization of gold nanorods and their application for photothermal cell damage. Int J Nanomedicine. 2011; 6:1825–31. [PubMed: 22114472]
25. Choi WI, Sahu A, Kim YH, Tae G. Photothermal cancer therapy and imaging based on gold nanorods. Ann Biomed Eng. 2012; 40(2):534–46. [PubMed: 21887589]
26. Gormley AJ, Greish K, Ray A, Robinson R, Gustafson JA, Ghandehari H. Gold nanorod mediated plasmonic photothermal therapy: a tool to enhance macromolecular delivery. Int J Pharm. 2011; 415(1–2):315–8. [PubMed: 21669265]
27. Ye E, Win KY, Tan HR, Lin M, Teng CP, Mlayah A, Han MY. Plasmonic gold nanocrosses with multidirectional excitation and strong photothermal effect. J Am Chem Soc. 2011; 133(22):8506–9. [PubMed: 21563806]
28. Choi WI, Kim JY, Kang C, Byeon CC, Kim YH, Tae G. Tumor regression in vivo by photothermal therapy based on gold-nanorod-loaded, functional nanocarriers. ACS Nano. 2011; 5(3):1995–2003. [PubMed: 21344891]
29. Ke H, Wang J, Dai Z, Jin Y, Qu E, Xing Z, Guo C, Yue X, Liu J. Gold-nanoshelled microcapsules: a theranostic agent for ultrasound contrast imaging and photothermal therapy. Angew Chem Int Ed Engl. 2011; 50(13):3017–21. [PubMed: 21404389]
30. Kirui DK, Krishnan S, Strickland AD, Batt CA. PAA-derived gold nanorods for cellular targeting and photothermal therapy. Macromol Biosci. 2011; 11(6):779–88. [PubMed: 21438153]
31. Goodrich GP, Bao L, Gill-Sharp K, Sang KL, Wang J, Payne JD. Photothermal therapy in a murine colon cancer model using near-infrared absorbing gold nanorods. J Biomed Opt. 2010; 15(1): 018001. [PubMed: 20210487]
32. Gobin AM, Watkins EM, Quevedo E, Colvin VL, West JL. Near-infrared-resonant gold/gold sulfide nanoparticles as a photothermal cancer therapeutic agent. Small. 2010; 6(6):745–52. [PubMed: 20183810]
33. Kirui DK, Rey DA, Batt CA. Gold hybrid nanoparticles for targeted phototherapy and cancer imaging. Nanotechnology. 2010; 21(10):105105. [PubMed: 20154383]
34. Dickerson EB, Dreaden EC, Huang X, El-Sayed IH, Chu H, Pushpanketh S, McDonald JF, El-Sayed MA. Gold nanorod assisted near-infrared plasmonic photothermal therapy (PPTT) of squamous cell carcinoma in mice. Cancer Lett. 2008; 269(1):57–66. [PubMed: 18541363]
35. Ramos J, Rege K. Transgene delivery using poly(amino ether)-gold nanorod assemblies. Biotechnol Bioeng. 2012; 109(5):1336–46. [PubMed: 22170455]

36. Zhang W, Meng J, Ji Y, Li X, Kong H, Wu X, Xu H. Inhibiting metastasis of breast cancer cells in vitro using gold nanorod-siRNA delivery system. Nanoscale. 2011; 3(9):3923–32. [PubMed: 21845256]
37. Kong WH, Bae KH, Jo SD, Kim JS, Park TG. Cationic lipid-coated gold nanoparticles as efficient and non-cytotoxic intracellular siRNA delivery vehicles. Pharm Res. 2012; 29(2):362–74. [PubMed: 21842305]
38. Bonoiu AC, Bergey EJ, Ding H, Hu R, Kumar R, Yong KT, Prasad PN, Mahajan S, Picchione KE, Bhattacharjee A, Ignatowski TA. Gold nanorod--siRNA induces efficient in vivo gene silencing in the rat hippocampus. Nanomedicine. 2011; 6(4):617–30. [PubMed: 21718174]
39. Kim EY, Schulz R, Swantek P, Kunstman K, Malim MH, Wolinsky SM. Gold nanoparticle-mediated gene delivery induces widespread changes in the expression of innate immunity genes. Gene Ther. 2012; 19(3):347–53. [PubMed: 21697957]
40. Lee SK, Han MS, Asokan S, Tung CH. Effective gene silencing by multilayered siRNA-coated gold nanoparticles. Small. 2011; 7(3):364–70. [PubMed: 21294265]
41. Kim DW, Kim JH, Park M, Yeom JH, Go H, Kim S, Han MS, Lee K, Bae J. Modulation of biological processes in the nucleus by delivery of DNA oligonucleotides conjugated with gold nanoparticles. Biomaterials. 2011; 32(10):2593–604. [PubMed: 21251710]
42. Guo S, Huang Y, Jiang Q, Sun Y, Deng L, Liang Z, Du Q, Xing J, Zhao Y, Wang PC, Dong A, Liang XJ. Enhanced gene delivery and siRNA silencing by gold nanoparticles coated with charge-reversal polyelectrolyte. ACS Nano. 2010; 4(9):5505–11. [PubMed: 20707386]
43. Kirkland-York S, Zhang Y, Smith AE, York AW, Huang F, McCormick CL. Tailored design of Au nanoparticle-siRNA carriers utilizing reversible addition-fragmentation chain transfer polymers. Biomacromolecules. 2010; 11(4):1052–9. [PubMed: 20337403]
44. Song WJ, Du JZ, Sun TM, Zhang PZ, Wang J. Gold nanoparticles capped with polyethyleneimine for enhanced siRNA delivery. Small. 2010; 6(2):239–46. [PubMed: 19924738]
45. Bonoiu AC, Mahajan SD, Ding H, Roy I, Yong KT, Kumar R, Hu R, Bergey EJ, Schwartz SA, Prasad PN. Nanotechnology approach for drug addiction therapy: gene silencing using delivery of gold nanorod-siRNA nanoplex in dopaminergic neurons. Proc Natl Acad Sci U S A. 2009; 106(14):5546–50. [PubMed: 19307583]
46. Ghosh PS, Kim CK, Han G, Forbes NS, Rotello VM. Efficient gene delivery vectors by tuning the surface charge density of amino acid-functionalized gold nanoparticles. ACS Nano. 2008; 2(11): 2213–8. [PubMed: 19206385]
47. Shukla R, Chanda N, Zambre A, Upendran A, Katti K, Kulkarni RR, Nune SK, Casteel SW, Smith CJ, Vimal J, Boote E, Robertson JD, Kan P, Engelbrecht H, Watkinson LD, Carmack TL, Lever JR, Cutler CS, Caldwell C, Kannan R, Katti KV. Laminin receptor specific therapeutic gold nanoparticles (198AuNP-EGCg) show efficacy in treating prostate cancer. Proc Natl Acad Sci U S A. 2012; 109(31):12426–31. [PubMed: 22802668]
48. http://www.fda.gov/MedicalDevices/ProductsandMedicalProcedures/DeviceApprovalsandClearances/510kClearances/ucm083781.htm
49. http://www.fda.gov/MedicalDevices/ProductsandMedicalProcedures/DeviceApprovalsandClearances/510kClearances/ucm083784.htm
50. Libutti SK, Paciotti GF, Byrnes AA, Alexander HR Jr, Gannon WE, Walker M, Seidel GD, Yuldasheva N, Tamarkin L. Phase I and pharmacokinetic studies of CYT-6091, a novel PEGylated colloidal gold-rhTNF nanomedicine. Clin Cancer Res. 2010; 16(24):6139–49. [PubMed: 20876255]
51. Pilot Study of AuroLase(tm) Therapy in Refractory and/or Recurrent Tumors of the Head and Neck. http://clinicaltrials.gov/ct2/show/NCT00848042 Clinical trial identifier: NCT00848042
52. Plasmonic Nanophotothermic Therapy of Atherosclerosis (NANOM). http://clinicaltrials.gov/ct2/show/NCT01270139 Clinical trial identifier: NCT01270139
53. Plasmonic Photothermal and Stem Cell Therapy of Atherosclerosis Versus Biodegradable Stenting (NANOM2). http://clinicaltrials.gov/ct2/show/NCT01436123 Clinical trial identifier: NCT01436123

54. von Maltzahn G, Park JH, Agrawal A, Bandaru NK, Das SK, Sailor MJ, Bhatia SN. Computationally guided photothermal tumor therapy using long-circulating gold nanorod antennas. Cancer Res. 2009; 69(9):3892–900. [PubMed: 19366797]
55. Heo DN, Yang DH, Moon HJ, Lee JB, Bae MS, Lee SC, Lee WJ, Sun IC, Kwon IK. Gold nanoparticles surface-functionalized with paclitaxel drug and biotin receptor as theranostic agents for cancer therapy. Biomaterials. 2012; 33(3):856–66. [PubMed: 22036101]
56. Brust M, Walker M, Bethell D, Schiffrin DJ, Whyman R. Synthesis of thiol-derivatised gold nanoparticles in a two-phase liquid–liquid system. Chem Commun. 1994:801–802.
57. Turkevich J, Stevenson PC, Hillier J. A study of the nucleation and growth processes in the synthesis of colloidal gold. Discuss Faraday Soc. 1951; 11:55–75.
58. Frens G. Controlled nulceation for regulation of particle size in monodisperse gold suspensions. Nat Phys Sci. 1973; 241(105):20–22.
59. Hostetler MJ, Wingate JE, Zhong CJ, Harris JE, Vachet RW, Clark MR, Londono JD, Green SJ, Stokes JJ, Wignall GD, Glish GL, Porter MD, Evans ND, Murray RW. Alkanethiolate gold cluster molecules with core diameters from 1.5 to 5. 2 nm: core and monolayer properties as a function of core size. Langmuir. 1998; 14:17–30.
60. Mulder WJM, Strijkers GJ, Van Tilborg GAF, Cormode DP, Fayad ZA, Nicolay K. Nanoparticulate assemblies of amphiphiles and diagnostically active materials for multimodality imaging. Acc Chem Res. 2009; 42(7):904–914. [PubMed: 19435319]
61. Panda T, Deepa K. Biosynthesis of gold nanoparticles. J Nanosci Nanotechnol. 2011; 11(12): 10279–94. [PubMed: 22408900]
62. Chandran SP, Chaudhary M, Pasricha R, Ahmad A, Sastry M. Synthesis of gold nanotriangles and silver nanoparticles using Aloe vera plant extract. Biotechnol Prog. 2006; 22(2):577–83. [PubMed: 16599579]
63. Firestone MA, Dietz ML, Seifert S, Trasobares S, Miller DJ, Zaluzec NJ. Ionogel-templated synthesis and organization of anisotropic gold nanoparticles. Small. 2005; 1(7):754–60. [PubMed: 17193519]
64. Shankar SS, Bhargava S, Sastry M. Synthesis of gold nanospheres and nanotriangles by the Turkevich approach. J Nanosci Nanotechnol. 2005; 5(10):1721–7. [PubMed: 16245535]
65. Skrabalak SE, Chen J, Sun Y, Lu X, Au L, Cobley CM, Xia Y. Gold nanocages: synthesis, properties, and applications. Acc Chem Res. 2008; 41(12):1587–95. [PubMed: 18570442]
66. Yuan H, Khoury CG, Hwang H, Wilson CM, Grant GA, Vo-Dinh T. Gold nanostars: surfactant-free synthesis, 3D modelling, and two-photon photoluminescence imaging. Nanotechnology. 2012; 23(7):075102. [PubMed: 22260928]
67. Cormode DP, Sanchez-Gaytan BL, Mieszawska AJ, Fayad ZA, Mulder WJ. Inorganic nanocrystals as contrast agents in MRI: synthesis, coating and introducing multifunctionality. NMR Biomed. in press.
68. Daniel MC, Astruc D. Gold nanoparticles: assembly, supramolecular chemistry, quantum-size-related properties, and applications toward biology, catalysis, and nanotechnology. Chem Rev. 2004; 104:293–346. [PubMed: 14719978]
69. Hostetler MJ, Wingate JE, Zhong CJ, Harris JE, Vachet RW, Clark MR, Londono JD, Green SJ, Stokes JJ, Wignall GD, Glish GL, Porter MD, Evans ND, Murray RW. Monolayers in three dimensions: synthesis and electrochemistry of ω-functionalized alkanethiolate-stabilized gold cluster compounds. Langmuir. 1998; 14:17–30.
70. Cormode DP, Skajaa T, Fayad ZA, Mulder WJM. Nanotechnology in medical imaging: probe design and applications. Arterioscler Thromb Vasc Biol. 2009; 29:992–1000. [PubMed: 19057023]
71. Boca SC, Astilean S. Detoxification of gold nanorods by conjugation with thiolated poly(ethylene glycol) and their assessment as SERS-active carriers of Raman tags. Nanotechnology. 2010; 21(23):235601. [PubMed: 20463383]
72. Niidome T, Akiyama Y, Yamagata M, Kawano T, Mori T, Niidome Y, Katayama Y. Poly(ethylene glycol)-modified gold nanorods as a photothermal nanodevice for hyperthermia. J Biomater Sci Polym Ed. 2009; 20(9):1203–15. [PubMed: 19520008]

73. Niidome T, Yamagata M, Okamoto Y, Akiyama Y, Takahashi H, Kawano T, Katayama Y, Niidome Y. PEG-modified gold nanorods with a stealth character for in vivo applications. J Control Release. 2006; 114(3):343–7. [PubMed: 16876898]
74. Yue Y, Liu TY, Li HW, Liu Z, Wu Y. Microwave-assisted synthesis of BSA-protected small gold nanoclusters and their fluorescence-enhanced sensing of silver(I) ions. Nanoscale. 2012; 4(7): 2251–4. [PubMed: 22382936]
75. Vanderkooy A, Chen Y, Gonzaga F, Brook MA. Silica shell/gold core nanoparticles: correlating shell thickness with the plasmonic red shift upon aggregation. ACS Appl Mater Interfaces. 2011; 3(10):3942–7. [PubMed: 21882833]
76. Kojima C, Hirano Y, Yuba E, Harada A, Kono K. Preparation and characterization of complexes of liposomes with gold nanoparticles. Colloids Surf B Biointerfaces. 2008; 66(2):246–52. [PubMed: 18723331]
77. Aryal S, Pilla S, Gong S. Multifunctional nano-micelles formed by amphiphilic gold-polycaprolactone-methoxy poly(ethylene glycol) (Au-PCL-MPEG) nanoparticles for potential drug delivery applications. J Nanosci Nanotechnol. 2009; 9(10):5701–8. [PubMed: 19908441]
78. Mieszawska AJ, Gianella A, Cormode DP, Zhao Y, Meijerink A, Langer R, Farokhzad OC, Fayad ZA, Mulder WJ. Engineering of lipid-coated PLGA nanoparticles with a tunable payload of diagnostically active nanocrystals for medical imaging. Chem Commun. 2012; 48(47):5835–7.
79. Wang H, Zheng L, Guo R, Peng C, Shen M, Shi X, Zhang G. Dendrimer-entrapped gold nanoparticles as potential CT contrast agents for blood pool imaging. Nanoscale Res Lett. 2012; 7:190. [PubMed: 22429280]
80. Peng C, Zheng L, Chen Q, Shen M, Guo R, Wang H, Cao X, Zhang G, Shi X. PEGylated dendrimer-entrapped gold nanoparticles for in vivo blood pool and tumor imaging by computed tomography. Biomaterials. 2012; 33(4):1107–19. [PubMed: 22061490]
81. Maeda H, Wu J, Sawa T, Matsumura Y, Hori K. Tumor vascular permeability and the EPR effect in macromolecular therapeutics: a review. J Control Release. 2000; 65:271–284. [PubMed: 10699287]
82. Cormode DP, Skajaa T, van Schooneveld MM, Koole R, Jarzyna P, Lobatto ME, Calcagno C, Barazza A, Gordon RE, Zanzonico P, Fisher EA, Fayad ZA, Mulder WJ. Nanocrystal core high-density lipoproteins: a multimodality contrast agent platform. Nano Lett. 2008; 8(11):3715–23. [PubMed: 18939808]
83. Kumar A, Ma H, Zhang X, Huang K, Jin S, Liu J, Wei T, Cao W, Zou G, Liang XJ. Gold nanoparticles functionalized with therapeutic and targeted peptides for cancer treatment. Biomaterials. 2012; 33(4):1180–9. [PubMed: 22056754]
84. Arifin DR, Long CM, Gilad AA, Alric C, Roux S, Tillement O, Link TW, Arepally A, Bulte JWM. Trimodal gadolinium-gold microcapsules containing pancreatic islet cells restore normoglycemia in diabetic mice and can be tracked by using US, CT, and positive-contrast MR imaging. Radiology. 2011; 260(3):790–798. [PubMed: 21734156]
85. Cai QY, Kim SH, Choi KS, Kim SY, Byun SJ, Kim KW, Park SH, Juhng SK, Yoon KH. Colloidal gold nanoparticles as a blood-pool contrast agent for X-ray computed tomography in mice. Invest Radiol. 2007; 42(12):797–806. [PubMed: 18007151]
86. Hainfeld JF, Slatkin DN, Focella TM, Smilowitz HM. Gold nanoparticles: a new X-ray contrast agent. Br J Radiol. 2006; 79(939):248–53. [PubMed: 16498039]
87. Xu C, Tung GA, Sun S. Size and Concentration Effect of Gold Nanoparticles on X-ray Attenuation As Measured on Computed Tomography. Chem Mater. 2008; 20(13):4167–4169. [PubMed: 19079760]
88. Kim D, Park S, Lee JH, Jeong YY, Jon S. Antibiofouling polymer-coated gold nanoparticles as a contrast agent for in vivo X-ray computed tomography imaging. J Am Chem Soc. 2007; 129(24): 7661–5. [PubMed: 17530850]
89. Menk RH, Schultke E, Hall C, Arfelli F, Astolfo A, Rigon L, Round A, Ataelmannan K, MacDonald SR, Juurlink BH. Gold nanoparticle labeling of cells is a sensitive method to investigate cell distribution and migration in animal models of human disease. Nanomedicine. 2011; 7(5):647–54. [PubMed: 21333753]

90. Popovtzer R, Agrawal A, Kotov NA, Popovtzer A, Balter J, Carey TE, Kopelman R. Targeted gold nanoparticles enable molecular CT imaging of cancer. Nano Lett. 2008; 8(12):4593–6. [PubMed: 19367807]

91. Aydogan B, Li J, Rajh T, Chaudhary A, Chmura SJ, Pelizzari C, Wietholt C, Kurtoglu M, Redmond P. AuNP-DG: deoxyglucose-labeled gold nanoparticles as X-ray computed tomography contrast agents for cancer imaging. Mol Imaging Biol. 2010; 12(5):463–7. [PubMed: 20237857]

92. Narayanan S, Sathy BN, Mony U, Koyakutty M, Nair SV, Menon D. Biocompatible magnetite/gold nanohybrid contrast agents via green chemistry for MRI and CT bioimaging. ACS Appl Mater Interfaces. 2011; 4(1):251–60. [PubMed: 22103574]

93. Li J, Chaudhary A, Chmura SJ, Pelizzari C, Rajh T, Wietholt C, Kurtoglu M, Aydogan B. A novel functional CT contrast agent for molecular imaging of cancer. Phys Med Biol. 2010; 55(15):4389–97. [PubMed: 20647599]

94. Reuveni T, Motiei M, Romman Z, Popovtzer A, Popovtzer R. Targeted gold nanoparticles enable molecular CT imaging of cancer: an in vivo study. Int J Nanomedicine. 2011; 6:2859–64. [PubMed: 22131831]

95. Jackson PA, Rahman WN, Wong CJ, Ackerly T, Geso M. Potential dependent superiority of gold nanoparticles in comparison to iodinated contrast agents. Eur J Radiol. 2010; 75(1):104–9. [PubMed: 19406594]

96. Sun IC, Eun DK, Na JH, Lee S, Kim IJ, Youn IC, Ko CY, Kim HS, Lim D, Choi K, Messersmith PB, Park TG, Kim SY, Kwon IC, Kim K, Ahn CH. Heparin-coated gold nanoparticles for liver-specific CT imaging. Chemistry. 2009; 15(48):13341–7. [PubMed: 19902441]

97. Sun IC, Eun DK, Koo H, Ko CY, Kim HS, Yi DK, Choi K, Kwon IC, Kim K, Ahn CH. Tumor-targeting gold particles for dual computed tomography/optical cancer imaging. Angew Chem Int Ed Engl. 2011; 50(40):9348–51. [PubMed: 21948430]

98. Kim D, Jeong YY, Jon S. A drug-loaded aptamer-gold nanoparticle bioconjugate for combined CT imaging and therapy of prostate cancer. ACS Nano. 2010; 4(7):3689–96. [PubMed: 20550178]

99. Hainfeld JF, O'Connor MJ, Dilmanian FA, Slatkin DN, Adams DJ, Smilowitz HM. Micro-CT enables microlocalisation and quantification of Her2-targeted gold nanoparticles within tumour regions. Br J Radiol. 2011; 84(1002):526–33. [PubMed: 21081567]

100. van Schooneveld MM, Cormode DP, Koole R, van Wijngaarden JT, Calcagno C, Skajaa T, Hilhorst J, Hart DC, Fayad ZA, Mulder WJM, Meijerink A. A fluorescent, paramagnetic and PEGylated gold/silica nanoparticle for MRI, CT and fluorescence imaging. Contrast Media Mol Imaging. 2010; 5(4):231–236. [PubMed: 20812290]

101. Alric C, Taleb J, Le Duc G, Mandon C, Billotey C, Le Meur-Herland A, Brochard T, Vocanson F, Janier M, Perriat P, Roux S, Tillement O. Gadolinium chelate coated gold nanoparticles as contrast agents for both X-ray computed tomography and magnetic resonance imaging. J Am Chem Soc. 2008; 130(18):5908–15. [PubMed: 18407638]

102. Roessl E, Brendel B, Engel KJ, Schlomka JP, Thran A, Proksa R. Sensitivity of photon-counting based K-edge imaging in X-ray computed tomography. IEEE Transactions On Medical Imaging. 2011; 30(9):1678–1690. [PubMed: 21507770]

103. Cormode DP, Roessl E, Thran A, Skajaa T, Gordon RE, Schlomka JP, Fuster V, Fisher EA, Mulder WJ, Proksa R, Fayad ZA. Atherosclerotic plaque composition: analysis with multicolor CT and targeted gold nanoparticles. Radiology. 2010; 256(3):774–82. [PubMed: 20668118]

104. Schirra CO, Senpan A, Roessl E, Thran A, Stacy AJ, Wu LN, Proksa R, Pan D. Second generation gold nanobeacons for robust K-edge imaging with multi-energy CT. J Mater Chem. 2012; 22(43):23071–23077. [PubMed: 23185109]

105. Pan D, Roessl E, Schlomka JP, Caruthers SD, Senpan A, Scott MJ, Allen JS, Zhang H, Hu G, Gaffney PJ, Choi ET, Rasche V, Wickline SA, Proksa R, Lanza GM. Computed tomography in color: nanoK-enhanced spectral CT molecular imaging. Angew Chem Int Ed. 2010; 49:9635–9639.

106. Pan D, Schirra CO, Senpan A, Schmieder AH, Stacy AJ, Roessl E, Thran A, Wickline SA, Proska R, Lanza GM. An early investigation of ytterbium nanocolloids for selective and quantitative "multicolor" spectral CT imaging. ACS Nano. 2012; 6(4):3364–3370. [PubMed: 22385324]

107. Mooradian A. Photoluminescence of metals. Phys Rev Lett. 1969; 22:185–187.

108. Link S, El-Sayed MA. Optical properties and ultrafast dynamics of metallic nanocrystals. Annu Rev Phys Chem. 2003; 54:331–66. [PubMed: 12626731]
109. Wang GTH, Murray RW, Menard L, Nuzzo RG. Near-IR luminescence of monolayer-protected metal clusters. J Am Chem Soc. 2005; 127:812–813. [PubMed: 15656600]
110. Wilcoxon JP, Martin JE, Parsapour F, Wiedenman B, Kelley DF. Photoluminescence from nanosize gold clusters. J Chem Phys. 1998; 108:9137–9143.
111. Hwang YN, Jeong DH, Shin HJ, Kim D, Jeoung SC, Han SH, Lee JS, Cho G. Femtosecond emission studies on gold nanoparticles. J Phys Chem B. 2002; 206:7581–7584.
112. Huang T, Murray RW. Visible luminescence of water-soluble monolayer-protected gold clusters. J Phys Chem B. 2001; 105:12498–12502.
113. Zheng J, Petty JT, Dickson RM. High quantum yield blue emission from water-soluble Au8 nanodots. J Am Chem Soc. 2003; 125:7780–7781. [PubMed: 12822978]
114. Eustis S, El-Sayed M. Aspect ratio dependence of the enhanced fluorescence intensity of gold nanorods: experimental and simulation study. J Phys Chem B. 2005; 109(34):16350–6. [PubMed: 16853078]
115. Ming T, Zhao L, Yang Z, Chen H, Sun L, Wang J, Yan C. Strong polarization dependence of plasmon-enhanced fluorescence on single gold nanorods. Nano Lett. 2009; 9(11):3896–903. [PubMed: 19754068]
116. Zheng J, Zhou C, Yu M, Liu J. Different sized luminescent gold nanoparticles. Nanoscale. 2012; 4(14):4073–83. [PubMed: 22706895]
117. Zhang Y, Yu J, Birch DJ, Chen Y. Gold nanorods for fluorescence lifetime imaging in biology. J Biomed Opt. 2010; 15(2):020504. [PubMed: 20459218]
118. Wang H, Huff TB, Zweifel DA, He W, Low PS, Wei A, Cheng JX. In vitro and in vivo two-photon luminescence imaging of single gold nanorods. Proc Natl Acad Sci U S A. 2005; 102(44): 15752–6. [PubMed: 16239346]
119. Durr NJ, Larson T, Smith DK, Korgel BA, Sokolov K, Ben-Yakar A. Two-photon luminescence imaging of cancer cells using molecularly targeted gold nanorods. Nano Lett. 2007; 7(4):941–5. [PubMed: 17335272]
120. Mohamed MB, Volkov V, Link S, El-Sayed MA. The 'lightning' gold nanorods: fluorescence enhancement of over a million compared to the gold metal. Chem Phys Lett. 2000; 317:517–523.
121. Li CZ, Male KB, Hrapovic S, Luong JH. Fluorescence properties of gold nanorods and their application for DNA biosensing. Chem Commun. 2005; (31):3924–6.
122. Tang SC, Fu YY, Lo WF, Hua TE, Tuan HY. Vascular labeling of luminescent gold nanorods enables 3-D microscopy of mouse intestinal capillaries. ACS Nano. 2010; 4(10):6278–84. [PubMed: 20886812]
123. Park J, Estrada A, Sharp K, Sang K, Schwartz JA, Smith DK, Coleman C, Payne JD, Korgel BA, Dunn AK, Tunnell JW. Two-photon-induced photoluminescence imaging of tumors using near-infrared excited gold nanoshells. Opt Express. 2008; 16(3):1590–9. [PubMed: 18542237]
124. Mecker LC, Tyner KM, Kauffman JF, Arzhantsev S, Mans DJ, Gryniewicz-Ruzicka CM. Selective melamine detection in multiple sample matrices with a portable Raman instrument using surface enhanced Raman spectroscopy-active gold nanoparticles. Anal Chim Acta. 2012; 733:48–55. [PubMed: 22704375]
125. Nehl CL, Liao H, Hafner JH. Optical properties of star-shaped gold nanoparticles. Nano Lett. 2006; 6(4):683–8. [PubMed: 16608264]
126. Schwartzberg AM, Olson TY, Talley CE, Zhang JZ. Synthesis, characterization, and tunable optical properties of hollow gold nanospheres. J Phys Chem B. 2006; 110(40):19935–44. [PubMed: 17020380]
127. Huang X, Jain PK, El-Sayed IH, El-Sayed MA. Gold nanoparticles: interesting optical properties and recent applications in cancer diagnostics and therapy. Nanomedicine. 2007; 2(5):681–93. [PubMed: 17976030]
128. Ungureanu C, Kroes R, Petersen W, Groothuis TA, Ungureanu F, Janssen H, van Leeuwen FW, Kooyman RP, Manohar S, van Leeuwen TG. Light interactions with gold nanorods and cells: implications for photothermal nanotherapeutics. Nano Lett. 2011; 11(5):1887–94. [PubMed: 21491868]

129. Kustner B, Gellner M, Schutz M, Schoppler F, Marx A, Strobel P, Adam P, Schmuck C, Schlucker S. SERS labels for red laser excitation: silica-encapsulated SAMs on tunable gold/silver nanoshells. Angew Chem Int Ed Engl. 2009; 48(11):1950–3. [PubMed: 19191355]

130. Nolan JP, Duggan E, Liu E, Condello D, Dave I, Stoner SA. Single cell analysis using surface enhanced Raman scattering (SERS) tags. Methods. 2012; 57(3):272–9. [PubMed: 22498143]

131. Lee S, Chon H, Lee M, Choo J, Shin SY, Lee YH, Rhyu IJ, Son SW, Oh CH. Surface-enhanced Raman scattering imaging of HER2 cancer markers overexpressed in single MCF7 cells using antibody conjugated hollow gold nanospheres. Biosens Bioelectron. 2009; 24(7):2260–3. [PubMed: 19056254]

132. Dinish US, Fu CY, Soh KS, Ramaswamy B, Kumar A, Olivo M. Highly sensitive SERS detection of cancer proteins in low sample volume using hollow core photonic crystal fiber. Biosens Bioelectron. 2012; 33(1):293–8. [PubMed: 22265083]

133. Lee M, Lee S, Lee JH, Lim HW, Seong GH, Lee EK, Chang SI, Oh CH, Choo J. Highly reproducible immunoassay of cancer markers on a gold-patterned microarray chip using surface-enhanced Raman scattering imaging. Biosens Bioelectron. 2010; 26(5):2135–41. [PubMed: 20926277]

134. Park H, Lee S, Chen L, Lee EK, Shin SY, Lee YH, Son SW, Oh CH, Song JM, Kang SH, Choo J. SERS imaging of HER2-overexpressed MCF7 cells using antibody-conjugated gold nanorods. Phys Chem Chem Phys. 2009; 11(34):7444–9. [PubMed: 19690717]

135. Maiti KK, Dinish US, Fu CY, Lee JJ, Soh KS, Yun SW, Bhuvaneswari R, Olivo M, Chang YT. Development of biocompatible SERS nanotag with increased stability by chemisorption of reporter molecule for in vivo cancer detection. Biosens Bioelectron. 2010; 26(2):398–403. [PubMed: 20801634]

136. Jiang L, Qian J, Cai F, He S. Raman reporter-coated gold nanorods and their applications in multimodal optical imaging of cancer cells. Anal Bioanal Chem. 2011; 400(9):2793–800. [PubMed: 21455653]

137. Schutz M, Steinigeweg D, Salehi M, Kompe K, Schlucker S. Hydrophilically stabilized gold nanostars as SERS labels for tissue imaging of the tumor suppressor p63 by immuno-SERS microscopy. Chem Commun. 2011; 47(14):4216–8.

138. Ock K, Jeon WI, Ganbold EO, Kim M, Park J, Seo JH, Cho K, Joo SW, Lee SY. Real-time monitoring of glutathione-triggered thiopurine anticancer drug release in live cells investigated by surface-enhanced Raman scattering. Anal Chem. 2012; 84(5):2172–8. [PubMed: 22280519]

139. Fujita K, Ishitobi S, Hamada K, Smith NI, Taguchi A, Inouye Y, Kawata S. Time-resolved observation of surface-enhanced Raman scattering from gold nanoparticles during transport through a living cell. J Biomed Opt. 2009; 14(2):024038. [PubMed: 19405766]

140. Eliasson C, Loren A, Engelbrektsson J, Josefson M, Abrahamsson J, Abrahamsson K. Surface-enhanced Raman scattering imaging of single living lymphocytes with multivariate evaluation. Spectrochim Acta A Mol Biomol Spectrosc. 2005; 61(4):755–60. [PubMed: 15649811]

141. Qian X, Peng XH, Ansari DO, Yin-Goen Q, Chen GZ, Shin DM, Yang L, Young AN, Wang MD, Nie S. In vivo tumor targeting and spectroscopic detection with surface-enhanced Raman nanoparticle tags. Nat Biotech. 2008; 26(1):83–90.

142. Kircher MF, de la Zerda A, Jokerst JV, Zavaleta CL, Kempen PJ, Mittra E, Pitter K, Huang R, Campos C, Habte F, Sinclair R, Brennan CW, Mellinghoff IK, Holland EC, Gambhir SS. A brain tumor molecular imaging strategy using a new triple-modality MRI-photoacoustic-Raman nanoparticle. Nat Med. 2012; 18(5):829–34. [PubMed: 22504484]

143. Manohar S, Ungureanu C, Van Leeuwen TG. Gold nanorods as molecular contrast agents in photoacoustic imaging: the promises and the caveats. Contrast Media Mol Imaging. 2011; 6(5):389–400. [PubMed: 22025339]

144. Yoon SJ, Mallidi S, Tam JM, Tam JO, Murthy A, Johnston KP, Sokolov KV, Emelianov SY. Utility of biodegradable plasmonic nanoclusters in photoacoustic imaging. Opt Lett. 2010; 35(22):3751–3. [PubMed: 21081985]

145. Andreev VG, Karabutov AA, Oraevsky AA. Detection of ultrawide-band ultrasound pulses in optoacoustic tomography. IEEE Trans Ultrason Ferroelectr Freq Control. 2003; 50(10):1383–90. [PubMed: 14609079]

146. Taruttis A, Herzog E, Razansky D, Ntziachristos V. Real-time imaging of cardiovascular dynamics and circulating gold nanorods with multispectral optoacoustic tomography. Opt Express. 2010; 18(19):19592–602. [PubMed: 20940855]

147. Chen YS, Frey W, Kim S, Kruizinga P, Homan K, Emelianov S. Silica-coated gold nanorods as photoacoustic signal nanoamplifiers. Nano Lett. 2011; 11(2):348–54. [PubMed: 21244082]

148. Agarwal A, Shao X, Rajian JR, Zhang H, Chamberland DL, Kotov NA, Wang X. Dual-mode imaging with radiolabeled gold nanorods. J Biomed Opt. 2011; 16(5):051307. [PubMed: 21639567]

149. Chen YS, Frey W, Kim S, Homan K, Kruizinga P, Sokolov K, Emelianov S. Enhanced thermal stability of silica-coated gold nanorods for photoacoustic imaging and image-guided therapy. Opt Express. 2010; 18(9):8867–78. [PubMed: 20588732]

150. Song KH, Wang LV. Deep reflection-mode photoacoustic imaging of biological tissue. J Biomed Opt. 2007; 12(6):060503. [PubMed: 18163798]

151. Ku G, Wang LV. Deeply penetrating photoacoustic tomography in biological tissues enhanced with an optical contrast agent. Opt Lett. 2005; 30(5):507–9. [PubMed: 15789718]

152. Moon GD, Choi SW, Cai X, Li W, Cho EC, Jeong U, Wang LV, Xia Y. A new theranostic system based on gold nanocages and phase-change materials with unique features for photoacoustic imaging and controlled release. J Am Chem Soc. 2011; 133(13):4762–5. [PubMed: 21401092]

153. Song KH, Kim C, Cobley CM, Xia Y, Wang LV. Near-infrared gold nanocages as a new class of tracers for photoacoustic sentinel lymph node mapping on a rat model. Nano Lett. 2009; 9(1): 183–8. [PubMed: 19072058]

154. Xia X, Yang M, Oetjen LK, Zhang Y, Li Q, Chen J, Xia Y. An enzyme-sensitive probe for photoacoustic imaging and fluorescence detection of protease activity. Nanoscale. 2011; 3(3): 950–3. [PubMed: 21225037]

155. Lu W, Melancon MP, Xiong C, Huang Q, Elliott A, Song S, Zhang R, Flores LG 2nd, Gelovani JG, Wang LV, Ku G, Stafford RJ, Li C. Effects of photoacoustic imaging and photothermal ablation therapy mediated by targeted hollow gold nanospheres in an orthotopic mouse xenograft model of glioma. Cancer Res. 2011; 71(19):6116–21. [PubMed: 21856744]

156. Song KH, Kim C, Maslov K, Wang LV. Noninvasive in vivo spectroscopic nanorod-contrast photoacoustic mapping of sentinel lymph nodes. Eur J Radiol. 2009; 70(2):227–31. [PubMed: 19269762]

157. Olafsson R, Bauer DR, Montilla LG, Witte RS. Real-time, contrast enhanced photoacoustic imaging of cancer in a mouse window chamber. Opt Express. 2010; 18(18):18625–32. [PubMed: 20940754]

158. Li PC, Wang CR, Shieh DB, Wei CW, Liao CK, Poe C, Jhan S, Ding AA, Wu YN. In vivo photoacoustic molecular imaging with simultaneous multiple selective targeting using antibody-conjugated gold nanorods. Opt Express. 2008; 16(23):18605–15. [PubMed: 19581946]

159. Agarwal A, Huang SW, O'Donnell M, Day KC, Day M, Kotov N, Ashkenazi S. Targeted gold nanorod contrast agent for prostate cancer detection by photoacoustic imaging. J Appl Phys. 2007; 102(6)

160. Lu W, Huang Q, Ku G, Wen X, Zhou M, Guzatov D, Brecht P, Su R, Oraevsky A, Wang LV, Li C. Photoacoustic imaging of living mouse brain vasculature using hollow gold nanospheres. Biomaterials. 2010; 31(9):2617–26. [PubMed: 20036000]

161. Wang B, Yantsen E, Larson T, Karpiouk AB, Sethuraman S, Su JL, Sokolov K, Emelianov SY. Plasmonic intravascular photoacoustic imaging for detection of macrophages in atherosclerotic plaques. Nano Lett. 2009; 9(6):2212–7. [PubMed: 18844426]

162. Pan D, Pramanik M, Wickline SA, Wang LV, Lanza GM. Recent advances in colloidal gold nanobeacons for molecular photoacoustic imaging. Contrast Media Mol Imaging. 2011; 6(5): 378–88. [PubMed: 22025338]

163. Pan D, Pramanik M, Senpan A, Allen JS, Zhang H, Wickline SA, Wang LV, Lanza GM. Molecular photoacoustic imaging of angiogenesis with integrin-targeted gold nanobeacons. FASEB J. 2011; 25(3):875–82. [PubMed: 21097518]

164. Pan D, Pramanik M, Senpan A, Yang X, Song KH, Scott MJ, Zhang H, Gaffney PJ, Wickline SA, Wang LV, Lanza GM. Molecular photoacoustic tomography with colloidal nanobeacons. Angew Chem Int Ed Engl. 2009; 48(23):4170–3. [PubMed: 19418503]

165. Nam SY, Ricles LM, Suggs LJ, Emelianov SY. In vivo ultrasound and photoacoustic monitoring of mesenchymal stem cells labeled with gold nanotracers. PLoS One. 2012; 7(5):e37267. [PubMed: 22615959]

166. Qu M, Mallidi S, Mehrmohammadi M, Truby R, Homan K, Joshi P, Chen YS, Sokolov K, Emelianov S. Magneto-photo-acoustic imaging. Biomed Opt Express. 2011; 2(2):385–96. [PubMed: 21339883]

167. Kim JW, Galanzha EI, Shashkov EV, Moon HM, Zharov VP. Golden carbon nanotubes as multimodal photoacoustic and photothermal high-contrast molecular agents. Nat Nanotechnol. 2009; 4(10):688–694. [PubMed: 19809462]

168. Jain PK, Lee KS, El-Sayed IH, El-Sayed MA. Calculated absorption and scattering properties of gold nanoparticles of different size, shape, and composition: applications in biological imaging and biomedicine. J Phys Chem B. 2006; 110(14):7238–48. [PubMed: 16599493]

169. He H, Xie C, Ren J. Nonbleaching fluorescence of gold nanoparticles and its applications in cancer cell imaging. Anal Chem. 2008; 80(15):5951–7. [PubMed: 18590338]

170. Craig GA, Allen PJ, Mason MD. Synthesis, characterization, and functionalization of gold nanoparticles for cancer imaging. Methods Mol Biol. 2010; 624:177–93. [PubMed: 20217596]

171. He H, Ren J. A novel evanescent wave scattering imaging method for single gold particle tracking in solution and on cell membrane. Talanta. 2008; 77(1):166–71. [PubMed: 18804615]

172. Zhang L, Zhen SJ, Sang Y, Li JY, Wang Y, Zhan L, Peng L, Wang J, Li YF, Huang CZ. Controllable preparation of metal nanoparticle/carbon nanotube hybrids as efficient dark field light scattering agents for cell imaging. Chem Commun. 2010; 46(24):4303–5.

173. Qian W, Huang X, Kang B, El-Sayed MA. Dark-field light scattering imaging of living cancer cell component from birth through division using bioconjugated gold nanoprobes. J Biomed Opt. 2010; 15(4):046025. [PubMed: 20799827]

174. Connor EE, Mwamuka J, Gole A, Murphy CJ, Wyatt MD. Gold nanoparticles are taken up by human cells but do not cause acute cytotoxicity. Small. 2005; 1(3):325–7. [PubMed: 17193451]

175. Daniel MC, Astruc D. Gold nanoparticles: assembly, supramolecular chemistry, quantum-size-related properties, and applications toward biology, catalysis, and nanotechnology. Chem Rev. 2004; 104(1):293–346. [PubMed: 14719978]

176. Love JC, Estroff LA, Kriebel JK, Nuzzo RG, Whitesides GM. Self-assembled monolayers of thiolates on metals as a form of nanotechnology. Chem Rev. 2005; 105(4):1103–69. [PubMed: 15826011]

177. Ghosh P, Han G, De M, Kim CK, Rotello VM. Gold nanoparticles in delivery applications. Adv Drug Deliv Rev. 2008; 60(11):1307–15. [PubMed: 18555555]

178. Kim CK, Ghosh P, Rotello VM. Multimodal drug delivery using gold nanoparticles. Nanoscale. 2009; 1(1):61–7. [PubMed: 20644861]

179. Mukhopadhyay A, Grabinski C, Afrooz AR, Saleh NB, Hussain S. Effect of gold nanosphere surface chemistry on protein adsorption and cell uptake in vitro. Appl Biochem Biotechnol. 2012; 167(2):327–37. [PubMed: 22547299]

180. Rana S, Bajaj A, Mout R, Rotello VM. Monolayer coated gold nanoparticles for delivery applications. Adv Drug Deliv Rev. 2012; 64(2):200–16. [PubMed: 21925556]

181. Wang F, Wang YC, Dou S, Xiong MH, Sun TM, Wang J. Doxorubicin-tethered responsive gold nanoparticles facilitate intracellular drug delivery for overcoming multidrug resistance in cancer cells. ACS Nano. 2011; 5(5):3679–92. [PubMed: 21462992]

182. Francois A, Laroche A, Pinaud N, Salmon L, Ruiz J, Robert J, Astruc D. Encapsulation of docetaxel into PEGylated gold nanoparticles for vectorization to cancer cells. ChemMedChem. 2011; 6(11):2003–8. [PubMed: 21834092]

183. Venkatpurwar V, Shiras A, Pokharkar V. Porphyran capped gold nanoparticles as a novel carrier for delivery of anticancer drug: in vitro cytotoxicity study. Int J Pharm. 2011; 409(1–2):314–20. [PubMed: 21376108]

184. You J, Zhang R, Zhang G, Zhong M, Liu Y, Van Pelt CS, Liang D, Wei W, Sood AK, Li C. Photothermal-chemotherapy with doxorubicin-loaded hollow gold nanospheres: A platform for near-infrared light-trigged drug release. J Control Release. 2012; 158(2):319–28. [PubMed: 22063003]

185. Pearson S, Scarano W, Stenzel MH. Micelles based on gold-glycopolymer complexes as new chemotherapy drug delivery agents. Chem Commun. 2012; 48(39):4695–7.

186. You J, Zhang G, Li C. Exceptionally high payload of doxorubicin in hollow gold nanospheres for near-infrared light-triggered drug release. ACS Nano. 2010; 4(2):1033–41. [PubMed: 20121065]

187. Tomuleasa C, Soritau O, Orza A, Dudea M, Petrushev B, Mosteanu O, Susman S, Florea A, Pall E, Aldea M, Kacso G, Cristea V, Berindan-Neagoe I, Irimie A. Gold nanoparticles conjugated with cisplatin/doxorubicin/capecitabine lower the chemoresistance of hepatocellular carcinoma-derived cancer cells. J Gastrointestin Liver Dis. 2012; 21(2):187–96. [PubMed: 22720309]

188. Paciotti GF, Myer L, Weinreich D, Goia D, Pavel N, McLaughlin RE, Tamarkin L. Colloidal gold: a novel nanoparticle vector for tumor directed drug delivery. Drug Deliv. 2004; 11(3):169–83. [PubMed: 15204636]

189. Shan Y, Luo T, Peng C, Sheng R, Cao A, Cao X, Shen M, Guo R, Tomas H, Shi X. Gene delivery using dendrimer-entrapped gold nanoparticles as nonviral vectors. Biomaterials. 2012; 33(10):3025–35. [PubMed: 22248990]

190. Chen CC, Lin YP, Wang CW, Tzeng HC, Wu CH, Chen YC, Chen CP, Chen LC, Wu YC. DNA-gold nanorod conjugates for remote control of localized gene expression by near infrared irradiation. J Am Chem Soc. 2006; 128(11):3709–15. [PubMed: 16536544]

191. Kim JH, Yeom JH, Ko JJ, Han MS, Lee K, Na SY, Bae J. Effective delivery of anti-miRNA DNA oligonucleotides by functionalized gold nanoparticles. J Biotechnol. 2011; 155(3):287–92. [PubMed: 21807040]

192. Lee SE, Sasaki DY, Perroud TD, Yoo D, Patel KD, Lee LP. Biologically functional cationic phospholipid-gold nanoplasmonic carriers of RNA. J Am Chem Soc. 2009; 131(39):14066–74. [PubMed: 19746908]

193. Conde J, Ambrosone A, Sanz V, Hernandez Y, Marchesano V, Tian F, Child H, Berry CC, Ibarra MR, Baptista PV, Tortiglione C, de la Fuente JM. Design of Multifunctional Gold Nanoparticles for In Vitro and In Vivo Gene Silencing. ACS Nano. 2012

194. Shim MS, Kim CS, Ahn YC, Chen Z, Kwon YJ. Combined multimodal optical imaging and targeted gene silencing using stimuli-transforming nanotheragnostics. J Am Chem Soc. 2010; 132(24):8316–24. [PubMed: 20518502]

195. Cui D, Huang P, Zhang C, Ozkan CS, Pan B, Xu P. Dendrimer-modified gold nanorods as efficient controlled gene delivery system under near-infrared light irradiation. J Control Release. 2011; 152(Suppl 1):e137–9. [PubMed: 22195805]

196. Wijaya A, Schaffer SB, Pallares IG, Hamad-Schifferli K. Selective release of multiple DNA oligonucleotides from gold nanorods. ACS Nano. 2009; 3(1):80–6. [PubMed: 19206252]

197. Guo R, Zhang L, Qian H, Li R, Jiang X, Liu B. Multifunctional nanocarriers for cell imaging, drug delivery, and near-IR photothermal therapy. Langmuir. 2010; 26(8):5428–34. [PubMed: 20095619]

198. Huang X, El-Sayed IH, Qian W, El-Sayed MA. Cancer cell imaging and photothermal therapy in the near-infrared region by using gold nanorods. J Am Chem Soc. 2006; 128(6):2115–20. [PubMed: 16464114]

199. Huang X, Qian W, El-Sayed IH, El-Sayed MA. The potential use of the enhanced nonlinear properties of gold nanospheres in photothermal cancer therapy. Lasers Surg Med. 2007; 39(9): 747–53. [PubMed: 17960762]

200. Loo C, Lowery A, Halas N, West J, Drezek R. Immunotargeted nanoshells for integrated cancer imaging and therapy. Nano Lett. 2005; 5(4):709–11. [PubMed: 15826113]

201. Li JL, Gu M. Surface plasmonic gold nanorods for enhanced two-photon microscopic imaging and apoptosis induction of cancer cells. Biomaterials. 2010; 31(36):9492–8. [PubMed: 20932571]

202. Wagner DS, Delk NA, Lukianova-Hleb EY, Hafner JH, Farach-Carson MC, Lapotko DO. The in vivo performance of plasmonic nanobubbles as cell theranostic agents in zebrafish hosting prostate cancer xenografts. Biomaterials. 2010; 31(29):7567–74. [PubMed: 20630586]

203. Chen J, Glaus C, Laforest R, Zhang Q, Yang M, Gidding M, Welch MJ, Xia Y. Gold nanocages as photothermal transducers for cancer treatment. Small. 2010; 6(7):811–7. [PubMed: 20225187]

204. Wang S, Chen KJ, Wu TH, Wang H, Lin WY, Ohashi M, Chiou PY, Tseng HR. Photothermal effects of supramolecularly assembled gold nanoparticles for the targeted treatment of cancer cells. Angew Chem Int Ed Engl. 2010; 49(22):3777–81. [PubMed: 20391446]

205. Park H, Yang J, Lee J, Haam S, Choi IH, Yoo KH. Multifunctional nanoparticles for combined doxorubicin and photothermal treatments. ACS Nano. 2009; 3(10):2919–26. [PubMed: 19772302]

206. Cho SH. Estimation of tumour dose enhancement due to gold nanoparticles during typical radiation treatments: a preliminary Monte Carlo study. Phys Med Biol. 2005; 50(15):N163–73. [PubMed: 16030374]

207. Begg AC, van der Kolk PJ, Emondt J, Bartelink H. Radiosensitization in vitro by cis-diammine (1,1-cyclobutanedicarboxylato) platinum(II) (carboplatin, JM8) and ethylenediammine-malonatoplatinum(II) (JM40). Radiother Oncol. 1987; 9(2):157–65. [PubMed: 3303163]

208. Mullenger L, Singh BB, Ormerod MG, Dean CJ. Chemical study of the radiosensitization of Micrococcus sodonensis by iodine compounds. Nature. 1967; 216(5113):372–4. [PubMed: 6053813]

209. Bernhard EJ, Mitchell JB, Deen D, Cardell M, Rosenthal DI, Brown JM. Reevaluating gadolinium(III) texaphyrin as a radiosensitizing agent. Cancer Res. 2000; 60(1):86–91. [PubMed: 10646858]

210. Jain S, Hirst DG, O'Sullivan JM. Gold nanoparticles as novel agents for cancer therapy. Br J Radiol. 2012; 85(1010):101–13. [PubMed: 22010024]

211. Hainfeld JF, Dilmanian FA, Slatkin DN, Smilowitz HM. Radiotherapy enhancement with gold nanoparticles. J Pharm Pharmacol. 2008; 60(8):977–85. [PubMed: 18644191]

212. Hainfeld JF, Slatkin DN, Smilowitz HM. The use of gold nanoparticles to enhance radiotherapy in mice. Phys Med Biol. 2004; 49(18):N309–15. [PubMed: 15509078]

213. Root SW, Andrews GA, Kniseley RM, Tyor MP. The distribution and radiation effects of intravenously administered colloidal Au198 in man. Cancer. 1954; 7(5):856–66. [PubMed: 13199762]

214. Rubin P, Levitt SH. The Response of Disseminated Reticulum Cell Sarcoma to the Intravenous Injection of Colloidal Radioactive Gold. J Nucl Med. 1964; 5:581–94. [PubMed: 14212184]

215. Jung JH, Jung SH, Kim SH, Choi SH. Synthesis and characterization of radioisotope nanospheres containing two gamma emitters. Appl Radiat Isot. 2012; 70(12):2677–2681. [PubMed: 23037922]

216. Huo Q, Litherland SA, Sullivan S, Hallquist H, Decker DA, Rivera-Ramirez I. Developing a nanoparticle test for prostate cancer scoring. J Transl Med. 2012; 10:44. [PubMed: 22404986]

217. You CC, Miranda OR, Gider B, Ghosh PS, Kim IB, Erdogan B, Krovi SA, Bunz UH, Rotello VM. Detection and identification of proteins using nanoparticle-fluorescent polymer 'chemical nose' sensors. Nat Nanotechnol. 2007; 2(5):318–23. [PubMed: 18654291]

218. Lytton-Jean AK, Han MS, Mirkin CA. Microarray detection of duplex and triplex DNA binders with DNA-modified gold nanoparticles. Anal Chem. 2007; 79(15):6037–41. [PubMed: 17614366]

219. Cormode DP, Davis JJ, Beer PD. Anion sensing porphyrin functionalized nanoparticles. J Inorg Organmet Polym. 2008; 18:32–40.

220. Virel A, Saa L, Pavlov V. Modulated growth of nanoparticles. Application for sensing nerve gases. Anal Chem. 2009; 81:268–272. [PubMed: 19049371]

221. Zheng G, Daniel WL, Mirkin CA. A new approach to amplified telomerase detection with polyvalent oligonucleotide nanoparticle conjugates. J Am Chem Soc. 2008; 130(30):9644–5. [PubMed: 18597453]

222. Kim YP, Daniel WL, Xia Z, Xie H, Mirkin CA, Rao J. Bioluminescent nanosensors for protease detection based upon gold nanoparticle-luciferase conjugates. Chem Commun. 2009; 46(1):76–8.

223. Lee JS, Ulmann PA, Han MS, Mirkin CA. A DNA-gold nanoparticle-based colorimetric competition assay for the detection of cysteine. Nano Lett. 2008; 8(2):529–33. [PubMed: 18205426]

224. Elghanian R, Storhoff JJ, Mucic RC, Letsinger RL, Mirkin CA. Selective colorimetric detection of polynucleotides based on the distance-dependent optical properties of gold nanoparticles. Science. 1997; 277(5329):1078–1081. [PubMed: 9262471]

225. Park SJ, Taton TA, Mirkin CA. Array-based electrical detection of DNA with nanoparticle probes. Science. 2002; 295(5559):1503–6. [PubMed: 11859188]

226. Conde J, de la Fuente JM, Baptista PV. RNA quantification using gold nanoprobes - application to cancer diagnostics. J Nanobiotechnology. 2010; 8:5. [PubMed: 20181241]

227. Cai X, Li W, Kim CH, Yuan Y, Wang LV, Xia Y. In vivo quantitative evaluation of the transport kinetics of gold nanocages in a lymphatic system by noninvasive photoacoustic tomography. ACS Nano. 2011; 5(12):9658–67. [PubMed: 22054348]

228. Thakor AS, Jokerst J, Zavaleta C, Massoud TF, Gambhir SS. Gold nanoparticles: a revival in precious metal administration to patients. Nano Lett. 2011; 11:4029–4036. [PubMed: 21846107]

229. Sahoo GP, Bar H, Bhui DK, Sarkar P, Samanta S, Pyne S, Ash S, Misra A. Synthesis and photo physical properties of star shaped gold nanoparticles. Colloids Surf A. 2011; 375(1–3):30–34.

230. Schneider GF, Subr V, Ulbrich K, Decher G. Multifunctional cytotoxic stealth nanoparticles. A model approach with potential for cancer therapy. Nano Lett. 2009; 9(2):636–642. [PubMed: 19170551]

231. Rasch MR, Rossinyol E, Hueso JL, Goodfellow BW, Arbiol J, Korgel BA. Hydrophobic gold nanoparticle self-assembly with phosphatidylcholine lipid: membrane- loaded and janus vesicles. Nano Lett. 2010; 10(9):3733–3739. [PubMed: 20731366]

232. Liu B, Xie J, Lee JY, Ting YP, Chen JP. Optimization of high-yield biological synthesis of single-crystalline gold nanoplates. J Phys Chem B. 2005; 109(32):15256–15263. [PubMed: 16852932]

233. Cho EC, Zhang Q, Xia Y. The effect of sedimentation and diffusion on cellular uptake of gold nanoparticles. Nat Nanotechnol. 2011; 6(6):385–391. [PubMed: 21516092]

234. Mulder WJM, Cormode DP, Hak S, Lobatto ME, Silvera S, Fayad ZA. Multimodality nanotracers for cardiovascular applications. Nat Clin Pract Cardiovasc Med. 2008; 5(S2):S103–S111. [PubMed: 18641599]

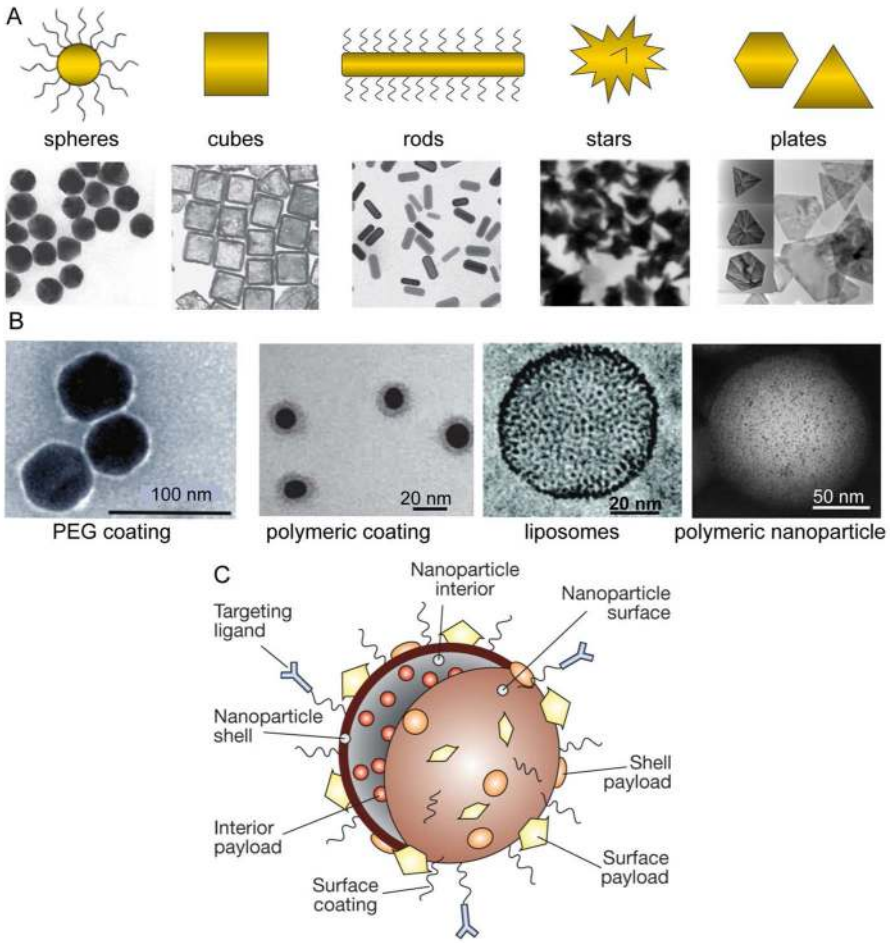

Figure 1.
Examples of different gold nanostructures (A) and examples of engineering of biocompatible gold nanoparticles through coating or encapsulation into carriers (B). (C) Aschematic depiction of gold nanoparticles for in vivo use. Figure adapted, with permission, from references [78, 141, 229–234].

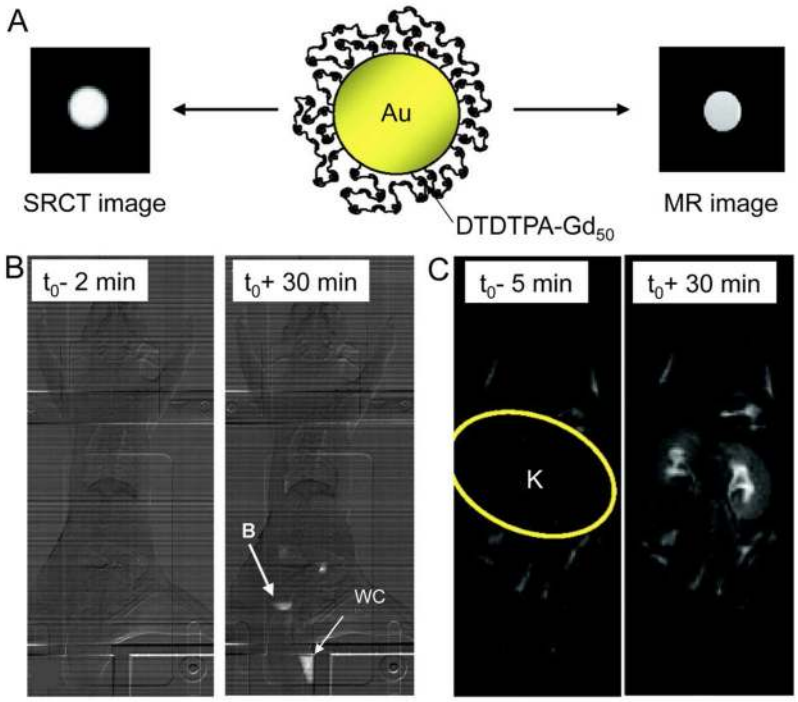

Figure 2.

Gold nanoparticles functionalized with Gd for dual modality imaging (SRCT and MRI). (A) The nanoparticle design with SRCT and MR images of vials of the agent to the left and right. (B) SRCT of a rat before (t = −2 min) and after injection (t = 30 min) of the AuNPs. (C) MR images of a rat before (t = −5 min) and after injection (t = 30 min) of the AuNPs. Abbreviations: B for bladder, K for kidneys, WC for the tube collecting the urine. Figure adapted, with permission, from reference [101].

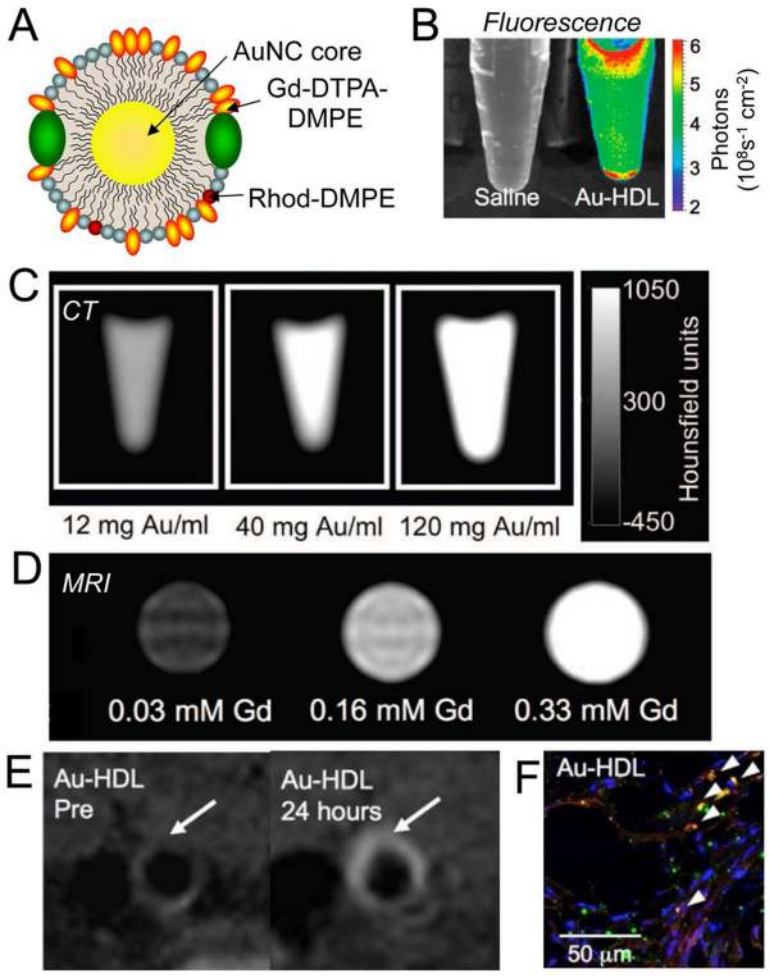

Figure 3.

A) A schematic depiction of a multimodality contrast agent with Au core providing contrast for CT and additional labels for fluorescent imaging (Rhodamine) and MRI (Gd) in the phospholipid coating. Fluorescence (B), CT (C) and MRI (D) phantoms demonstrating the contrast generating properties of the nanoparticle. E) MR images of an atherosclerotic mouse aorta pre- and 24 hours post-injection with AuNPs. F) Confocal microscopy image of the atherosclerotic plaque of a mouse, where nanoparticles are red, macrophages are green and nuclei are blue. Arrowheads indicate colocalization of nanoparticles and macrophages. Figure adapted, with permission, from reference [82].

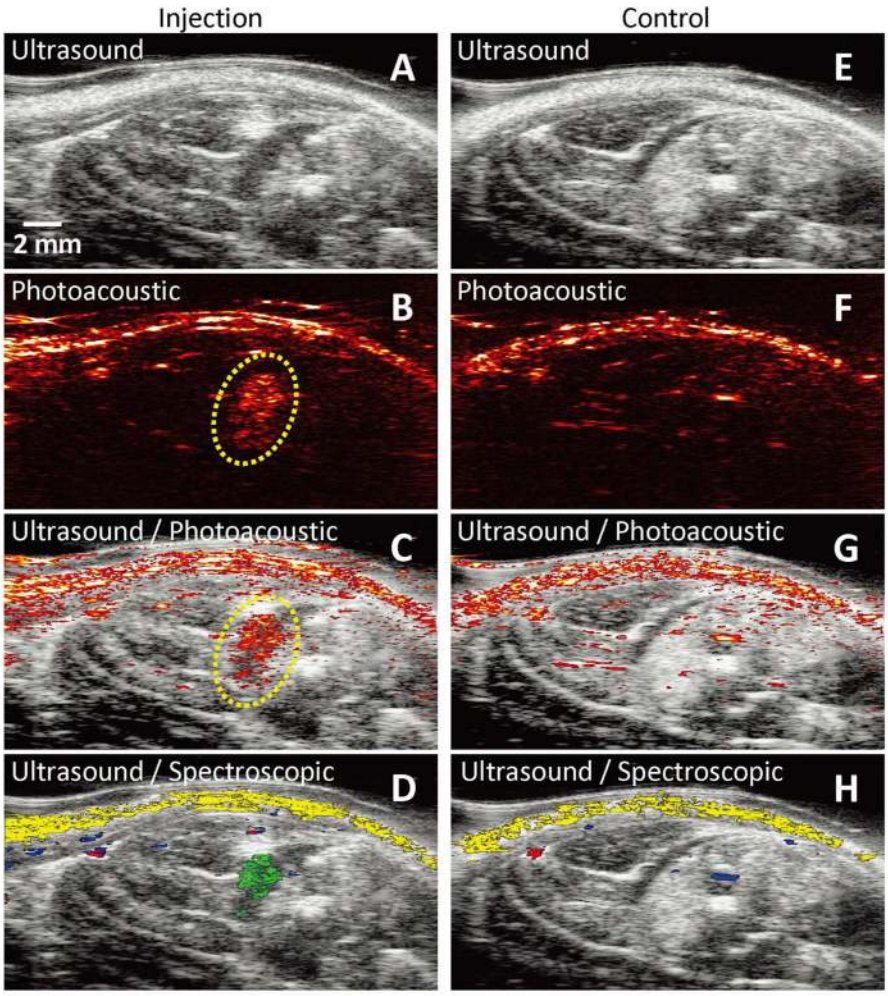

Figure 4.
In vivo photoacoustic imaging of stem cells via labeling with AuNPs. (A–D) Ultrasound, photoacoustic, ultrasound/photoacoustic overlay, and ultrasound/spectroscopic images of gel encapsulated stem cells labeled with AuNPs injected into a rat hind limb. (E–H) Corresponding images of a rat hind limb without injection. Figure adapted, with permission, from reference [165].

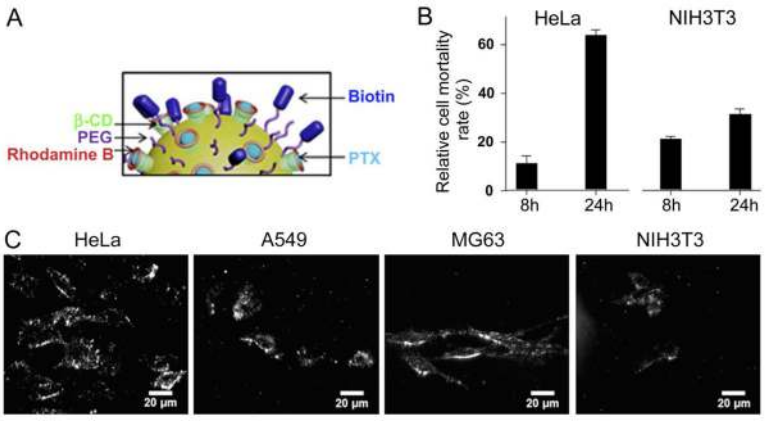

Figure 5.

A) Schematic depiction of gold nanoparticles functionalized with biotin, Rhodamine and paclitaxel (PTX) for cancer therapy. B) Cell mortality upon incubation with functionalized AuNPs. C) Dark field microscopy images of cells incubated with AuNPs. Figure adapted, with permission, from reference [55].

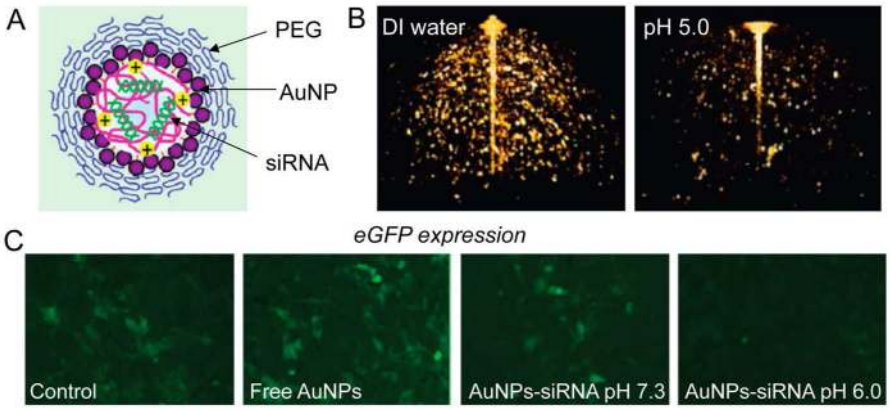

Figure 6.

Gold nanoparticles for imaging and gene silencing therapy. (A) Design of the nanoparticle. Upon hydrolysis under low pH, the nanoparticle releases the siRNA cargo. (B) Three dimensional optical coherence tomography images of the nanoparticles generated with AuNPs (lower intensity image on the right confirms NP disintegration at lower pH). (C) Fluorescence microscopy of eGFP-expressing NIH 3T3 cells reveals gene silencing when incubated with AuNP-siRNA at low pH. Figure adapted, with permission, from reference [194].

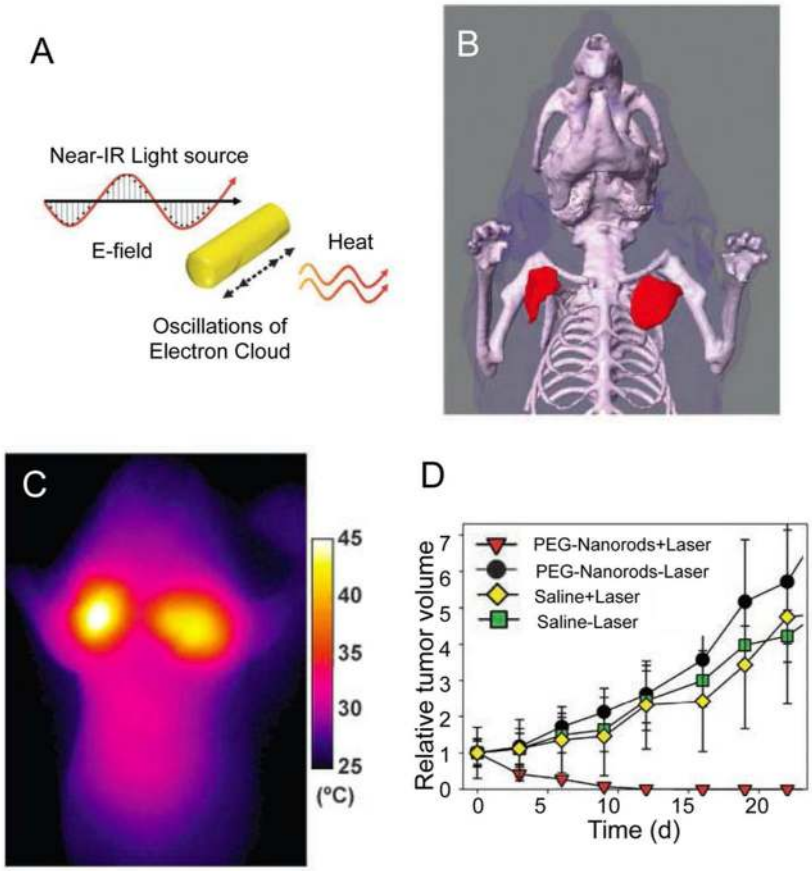

Figure 7.

AuNRs used for both imaging and therapy. A) Schematic depiction of photothermal heating of AuNRs. B) A three dimensional rendering of CT images of a mouse bearing two tumors on its chest, which had been injected with AuNRs. The location of the AuNRs is highlighted in red. C) Infra-red imaging of the mouse after NIR laser irradiation indicated the photothermal effect of the AuNRs. D) Tumor growth curves for mice treated with AuNRs and laser irradiation, compared with controls. Figure adapted, with permission, from reference [54].

Table 1

Summary of gold nanoparticle imaging applications, the properties required, the suitable gold nanoparticle types and pertinent references.

Imaging application	Property required, comments	Suitable gold nanoparticle type	Example references
X-ray imaging	X-ray absorption, no morphology/shape relationship, large nanoparticles have certain advantages due to high payload delivery	Any, spheres mostly used in practice	78–80, 82, 84–104
Fluorescence imaging	Rods and shells have inherent fluorescence. Other structures such as spheres can be made fluorescent via inclusion of other fluorophores	Rods, shells, labeled spheres	82, 100, 108–123
Surface enhanced Raman spectroscopy imaging	Strong electromagnetic field enhancement. Advantages to using structures such as stars, but much work has been done with spheres	Spheres, stars	8–11, 124–142
Photoacoustic imaging	Requires strong absorption in the NIR window	Cages, sphere clusters, rods, shells.	18–20, 143–167
Optical imaging	Strong light scattering. All structures scatter. Advantage of rods or shells is that the light used is in the NIR window. However, most studies have been done with visible light using spheres	Primarily spheres	12, 168–173

Table 2

Summary of gold nanoparticle therapy applications, the properties required, the suitable gold nanoparticle types and pertinent references.

Therapeutic application	Property required, comments	Suitable gold nanoparticle type	Example references
Drug delivery	Delivery depends mostly on surface properties. Shells have been used for photothermal triggered delivery	Any, spheres mostly used in practice	50, 55, 69, 83, 177–188
Nucleic acid delivery	Delivery depends mostly on surface properties. Rods have been used for photothermal triggered delivery	Any, spheres mostly used in practice	35–46, 189–196
Photothermal therapy	Strong absorption of light in the NIR window and efficient conversion of the light into heat	Rods, shells, cages	17, 21–34, 51–54, 197–205
Radiotherapy	Size/shape are not known to have any effect. Spheres have been used to date	Any, spheres used in practice	14, 47, 206, 210–215

Table 3

Summary of gold nanoparticle diagnostics applications, the properties required, the suitable gold nanoparticle types and pertinent references.

Diagnostic application	Property required, comments	Suitable gold nanoparticle type	Example references
Nucleic acid detection	Substantial change in light absorption properties upon nanoparticle aggregation	Any, spheres mostly used in practice	48, 49, 216, 218, 221, 223–226
Protein detection	Quenching of fluorescence at gold nanoparticle surface	Any, spheres used in practice	217